Disorders of lysosomes, peroxisomes, and mitochondria.

B E Kendall

AJNR Am J Neuroradiol 1992, 13 (2) 621-653
http://www.ajnr.org/content/13/2/621.citation

Disorders of Lysosomes, Peroxisomes, and Mitochondria

Brian E. Kendall[1]

From Department of Radiology, Hospital for Sick Children, London, England

Most inherited metabolic diseases affecting the nervous system are due to defective or deficient enzymes within lysosomes, peroxisomes, or mitochondria, but some are still of unknown etiology. In many of these diseases, the diagnosis can be strongly suspected from clinical findings and neurophysiologic tests. Confirmation is usually biochemical, though sometimes biopsy is necessary. In such circumstances, imaging may be unnecessary. However, when clinical presentation is atypical, the distribution of abnormalities on computed images of the brain and spinal contents may suggest the possibility of a particular type of metabolic disease.

In general, the relevant central nervous system (CNS) structures are more exactly shown by magnetic resonance (MR) imaging, especially when myelination is complete or well advanced. Serial imaging may elucidate prognosis or aid in management by monitoring the progress of disease or the response to therapy. Imaging may be indicated to explain unexpectedly rapid deterioration caused by complications of particular diseases such as hydrocephalus in mucopolysaccharidoses and Cockayne syndrome; foci of cerebral infarction or necrosis in MELAS, mucopolysaccharidoses, Menkes disease, Fabry disease, homocystinuria, ornithine carbamoyl transferase deficiency, and glycogen storage disease; and subdural effusion in Menkes disease and glutaric aciduria type 1.

[1] Address reprint requests to Dr Kendall at the Lysholm Radiological Department, the National Hospital for Neurology and Neurosurgery, Queen Square, London WCLN 3BG, England.

Index terms: Brain, metabolism; Lysosomes; Familial conditions; Pediatric neuroradiology; Peroxisomes, mitochondria

AJNR 13:621–653, Mar/Apr 1992 0195-6108/92/1302-0621

Lysosomal Disorders

Lysosomes are intracellular hydrolytic enzymes that are contained by membranes within the cytoplasm of most cells, but more abundantly in phagocytic cells, including leukocytes, tissue macrophages, and microglia. They aid in the digestion of phagocytosed particles. When the activity of a specific lysosome enzyme is deficient, a lysosomal storage disorder may result. These disorders are inherited in an autosomal recessive manner. Heterozygotes can generally be recognized by levels of enzyme activity that are low but less reduced than in homozygotes.

These disorders are classified on the basis of the abnormal materials stored in the lysosomes: in many of them, the nervous system is affected either directly or secondarily to involvement of the meninges or axial-skeletal structures.

Sphingolipidoses

Metachromatic Leukodystrophy. The commonest of these rare lysosomal conditions is characterized by a deficiency of the enzyme arylsulfatase A. This enzyme is necessary for the normal metabolism of sulfatides which are important constituents of the myelin sheath. In metachromatic leukodystrophy, sulfatide is stored within glial cells and neurones and gives the characteristic metachromatic reaction. The condition is diagnosed biochemically by lack of the enzyme in white blood cells and in the urine. False positives do occur, so when the clinical manifestations are atypical, the demonstration of increased amounts of sulfatide in the urine and/or neural tissues is confirmatory.

Clinically, the disease is subdivided according to the age at presentation. Signs may be evident at birth followed by a rapid downhill course, usually with convulsions, to early death. The

infantile type presents between 1 and 4 years of age with a painful polyneuropathy, ataxia, progressive retardation, and spastic tetraparesis. In juveniles, the disease is characterized by dementia and behavior disorders, with progression to spastic tetraparesis. Adult onset is rare, but it can present at any age with increasing dementia and spastic paraparesis.

Computed tomography (CT) and MR are most characteristic in the relatively common late infantile type. There is extensive symmetrical abnormality of the white matter of the centrum semiovale, which is low in density on CT (Fig. 1) and returns abnormal signal on MR; the peripheral cerebral white matter, including the arcuate fibers, tends to be spared until relatively late in the course of the disease (Fig. 2). These changes are due to demyelination and gliosis with no accompanying inflammatory reaction, so there is no abnormal enhancement. As the disease advances, there is loss of brain substance with increasing atrophy, and the density and signal changes become a less dramatic feature of the imaging studies.

Globoid Cell Leukodystrophy (Krabbe Disease). In this condition, deficiency of galactocerebroside betaglactosidase arrests the normal breakdown of cerebroside, which is a normal constituent of myelin. The diagnosis is made by showing deficiency of the enzyme in white blood cells. As soon as myelination commences and myelin turnover becomes necessary, the cerebroside accumulates in the lysosomes of histiocytes within the white matter, forming the globoid cells characteristic of the disease. In addition, galactosphin-

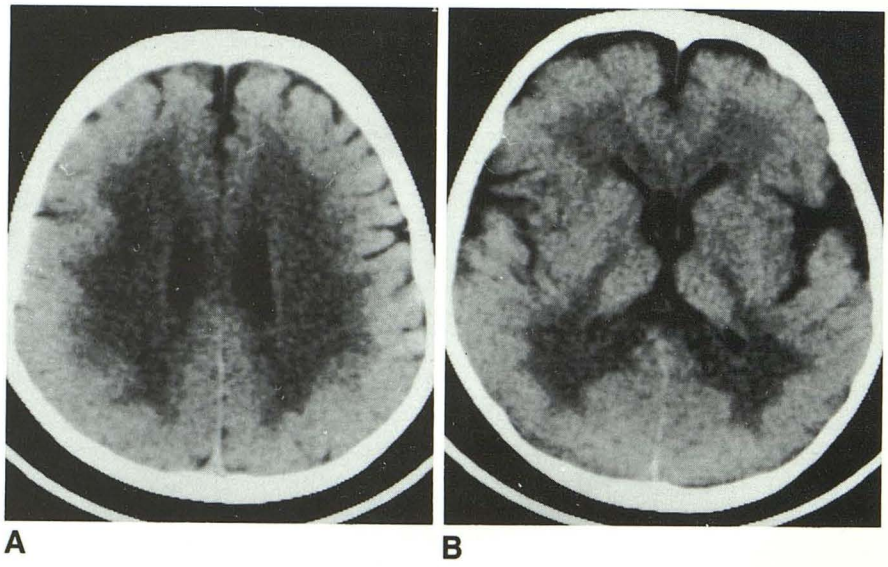

Fig. 1. Metachromatic leukodystrophy; axial CT sections through the corona radiata (*A*) and internal capsules (*B*). There is extensive low density throughout the deep cerebral white matter and involving the internal capsules with widening of the interhemispheric and Sylvian fissures due to mild cerebral atrophy.

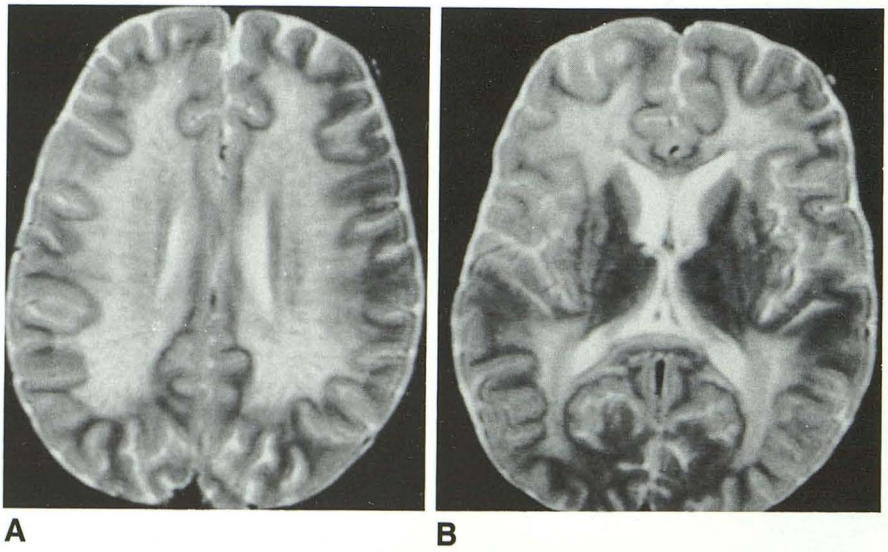

Fig. 2. Metachromatic leukodystrophy; axial T2 MR sections through the corona radiata (*A*) and internal capsules (*B*). There is high signal throughout the hemispheric white matter, sparing the arcuate fibers, the internal capsule, and the external capsule.

gosine is produced that may have toxic effects on oligodendrocytes, so that myelin production also may be defective.

The disease usually becomes evident between 1 and 6 months of age, but occasionally appears in the neonatal period. Clinically, psychomotor regression, hypertonicity, and pyrexia progress to blindness and opisthotonic postures, leading to a vegetative state and death within 1–3 years. Rarely, the disease presents later and then tends to run a more insidious course. The cerebrospinal fluid (CSF) has elevated protein and may contain a few monocytes.

The manifestations of the disease are confined to the nervous system; there is extensive cerebral demyelination, tending to spare the arcuate fibers, with secondary axon loss and gliosis. CT has shown high density within the thalami and caudate heads early in the course of the disease, together with low density in the white matter (Fig. 3) that may be confined to the parietal lobes. Slight peripheral enhancement has been described (1). On MR, there is nonspecific altered signal in the deep cerebral white matter, particularly of the parietal lobes (Fig. 4) (2). The thalami may show decreased T1 and normal or slightly decreased T2-weighted signal. As the disease advances there is diffuse cerebral atrophy.

Neimann-Pick Disease. This complex disease has at least five subtypes. In only two of these (types A and B) can a reliable diagnosis be made by enzymatic assay of white blood cells or fibroblasts. However, the disease is associated with

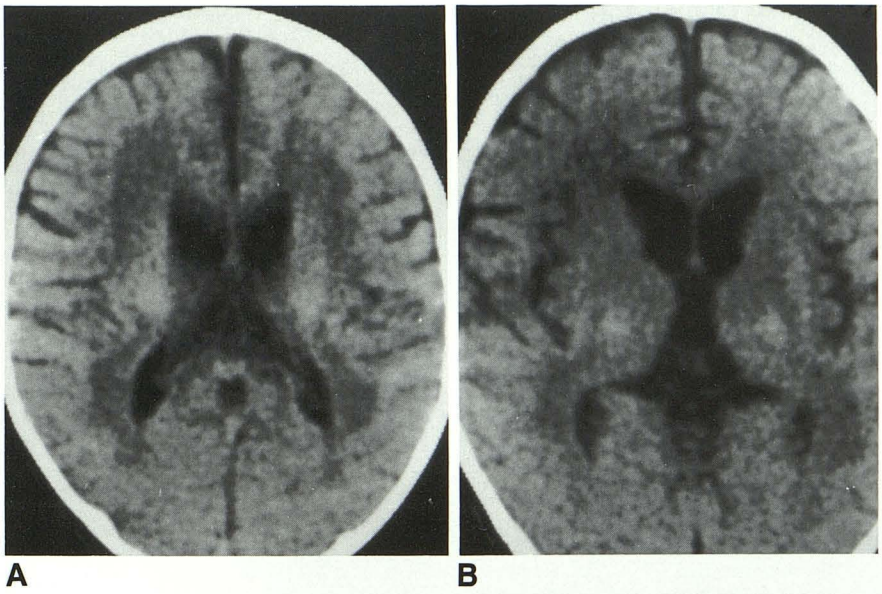

Fig. 3. Globoid cell leukodystrophy; axial CT sections through the corona radiata (*A*) and internal capsules (*B*). There is high density in the thalami and adjacent parts of the corona radiata, abnormally low density in the deep cerebral white matter, and mild diffuse cerebral atrophy.

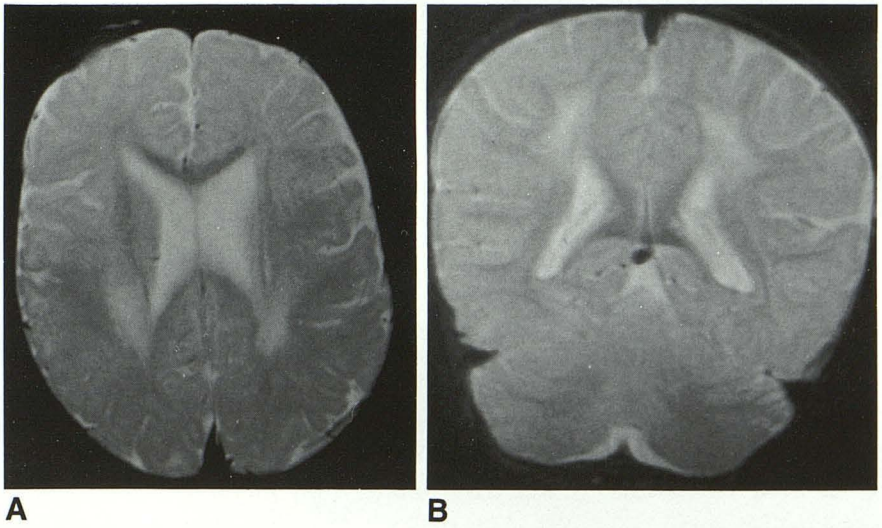

Fig. 4. Globoid cell leukodystrophy; cranial T2 MR in *A*, axial and *B*, coronal planes (Siemens magnatom 1.5 T, TR2000, TE90). There is symmetrical high signal confined to the parietal white matter.

diminished or absent sphingomyelinase activity and is characterized by the presence of sphingomyelin and cholesterol within the liposomes of all tissues. The disease commonly presents in the first few months of life, with enlargement of the liver, spleen, and lymph nodes, and swelling of lymphoid tissue in other organs as well.

Types A and C involve the CNS. Storage occurs within neurones and phagocytic cells in the white matter (Neimann-Pick cells), and in the leptomeninges and choroid plexuses; demyelination and gliosis are associated.

Fabry Disease. This X-linked disorder is due to deficiency of alphagalactosidase A, which results in accumulation of ceramide, trihexoside and dihexoside. Deposition within the walls of blood vessels and in epidermal cells is associated with the typical, though not specific, angiokeratoma corporis diffusum. Patients commonly—but not invariably—manifest skin rash and signs of autonomic dysfunction, with attacks of burning pain in the limbs or sensory neuropathy.

Involvement of the small arteries of the CNS causes stenosis and occlusion with multifocal small infarcts visible on CT or MR (Fig. 5). These may be asymptomatic or result in focal neurologic deficit, epilepsy, and/or dementia (3). Metabolic products may also accumulate in astrocytes and in neurones, particularly of the amygdala and hypothalamus, though this does not cause an abnormality evident on imaging.

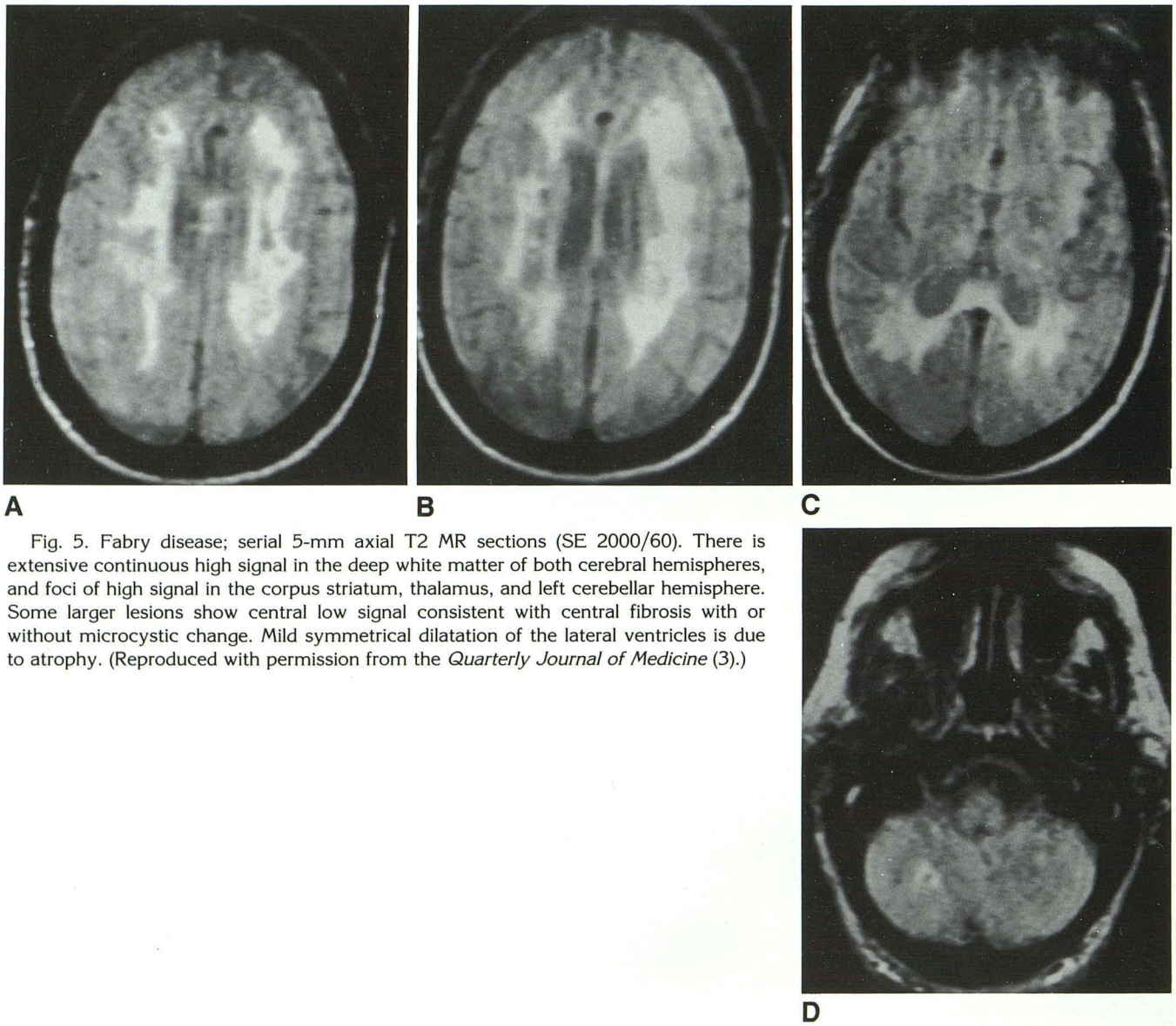

Fig. 5. Fabry disease; serial 5-mm axial T2 MR sections (SE 2000/60). There is extensive continuous high signal in the deep white matter of both cerebral hemispheres, and foci of high signal in the corpus striatum, thalamus, and left cerebellar hemisphere. Some larger lesions show central low signal consistent with central fibrosis with or without microcystic change. Mild symmetrical dilatation of the lateral ventricles is due to atrophy. (Reproduced with permission from the *Quarterly Journal of Medicine* (3).)

GM1 Gangliosidosis

Deficiency of betagalactosidase results in an accumulation of ganglioside in the lysosomes of cerebral and cerebellar neurones as well as in systemic organs. The latter is particularly pronounced in gangliosidosis GM1 type 1, also known as the infantile or pseudo-Hurler type because of clinical and skeletal resemblances to gargoylism. Neurologic symptoms are evident soon after birth, with retardation, incoordination, and spasticity, progressing to a decerebrate state with blindness and deafness leading to death before the age of 2 years. The diagnosis is made by estimating the betagalactosidase activity in leukcocytes in bone marrow samples. In GM1 gangliosidosis type 2, onset is later and systemic involvement, including dysostoses multiplex, is less marked. The child may survive up to the age of 10 years.

Computed imaging may be indicated for elucidation of retardation and macrocephaly, which is associated with the storage causing expansion of neurones. In type 1, demyelination and gliosis of the white matter causes low density on CT (Fig. 6) and altered signal on MR. Later stages of both type 1 and 2 show atrophy.

GM2 Gangliosidosis

This is a group of conditions in which there is deficiency of hexosaminidase enzymes. Diagnosis is confirmed by hexosaminidase assay of the leukocytes in blood samples. In Tay-Sachs disease, betahexosaminidase A alone is deficient, whereas in Sandhoff disease, betahexosaminidases A and B are both involved. The deficiency is associated with abnormal accumulation of GM2 ganglioside in nerve cells and in systemic organs.

In Tay-Sachs disease, retardation is usually evident by 6 months of age and is accompanied by motor defects, blindness, and epilepsy. The storage is accompanied by macrocephaly and by demyelination, oedema, spongiform degeneration, and gliosis of the white matter that may or may not involve the U fibers. The most typical finding on computed imaging is high density throughout the thalami on CT (4) and, sometimes, low signal on T2-weighted MR, possibly due to calcium deposition. There is low density and altered signal in white matter. Later there is atrophy, which is often most marked in the cerebellum.

In Sandhoff disease, the appearances in the CNS are similar, but there is more extensive storage of ganglioside in the liver and spleen.

In juvenile and adult varieties of the disease, the spinal cord is more extensively involved than the brain and may be markedly atrophic.

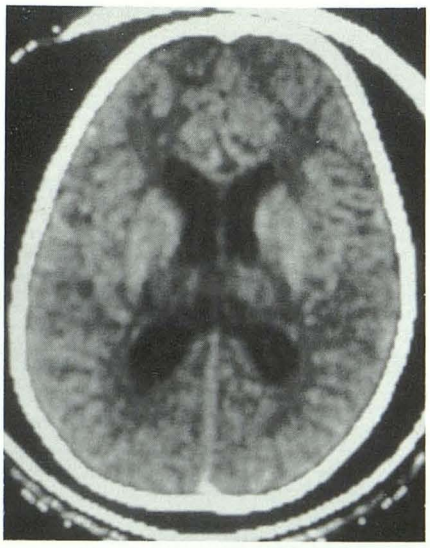

Fig. 6. GM1 gangliosidosis, type 2; 2-year-old child with mental retardation, ataxia, and macrocephaly. Axial CT; low density in the hemispheric white matter contrasts with high density in the basal ganglia. There is slight dilatation of the lateral ventricles.

Glycoproteinoses

Mannosidosis. This rare condition is associated with a defect in the activity of alphamannosidoses A and B that causes the intralysosomal accumulation of mannose-rich oligosaccharides in all cells. The diagnosis is made by showing typical vacuolation in the lymphocytes and decreased mannosidase activity in leukocytes. The disease varies in severity but results in some degree of mental retardation, Hurler-like facies, dysostosis multiplex, and thickening of the cranial vault. Storage in the nervous system occurs both peripherally and centrally, involving nerve cells of cortex, cerebellum, and spinal cord with gliosis and loss of myelin. Imaging studies show low density and altered signal in the parieto-occipital white matter (5), followed by cerebral and cerebellar atrophy.

Fucosidosis. This rare group of generalized storage disorders is due to deficiency of alphafucosidases that are necessary for the breakdown of glycoproteins, mucopolysaccharides, and mucolipids. This enzyme deficiency leads to the storage of ceramide in most cells. The disease is generally

evident in the first year of life and death occurs before 10 years, although the disease can first present later with survival into adult life. The systemic manifestations may simulate those of Hurler syndrome. Respiratory infection, cardiac failure, hepatosplenomegaly, and dysostosis multiplex are usual. Diagnosis is made biochemically from deficiency of alphafucosidase in leukocytes and urine.

Mental retardation progresses to complete decortication. Weakness and hypotonia are replaced by spasticity and hypertonia. Ceramide is stored in the cytoplasm of neurones and other cells, which become ballooned and then destroyed. This is accompanied by severe demyelination and gliosis, with extensive atrophy reflected in computed imaging studies.

Sialidosis. In this condition, a deficiency of the enzyme sialidase is associated with accumulation of sialic acid-containing glycoproteins and glycolipids in all tissues. It is diagnosed by assessment of enzyme levels in leukocytes and increased sialo-oligosaccharides in the urine. The disease presents in early life with myoclonus, seizures, and ataxia. Skeletal dysplasia, coarse facial features, and mental retardation are associated with cerebral atrophy in one variant.

Canavan Disease

This condition is associated with deficiency of the enzyme aspartoacylase. The resultant high concentration of *N*-acetylaspartic acid relative to choline and creatine can be demonstrated by spectroscopy in the brain substance. *N*-acetylaspartic acid is excreted in the urine (6).

The disease usually presents in infancy with retardation, hypotonia followed by spasticity, and eventually decortication with cortical blindness. There may be choreoathetoid movement and myoclonic seizures. An important diagnostic feature is macrocephaly. Death usually occurs before the age of 4 years. The disease less commonly presents at birth and proceeds to death within a few weeks. This disease may also present later and run a slower course without macrocephaly. Histology reveals vacuolation of cerebral white matter, and to a lesser extent of cortical gray matter, accompanied by astrocytic proliferation but no inflammatory reaction. Computed imaging displays (7) low density on CT (Fig. 7) and high signal on T2-weighted MR throughout the whole of the cerebral white matter. In the proper clinical context, these changes are characteristic, although not pathognomonic, of Canavan disease. In some cases the arcuate fibers appear to be involved early with centripetal spread, although in others the arcuate fibers are relatively spared (8). Particularly in rapidly progressive cases, the internal and external capsules are involved; cerebellar white matter is usually affected as well. There is no pathologic enhancement. As the disease progresses, atrophy becomes a conspicuous feature (Fig. 8).

Mucolipidosis

I-Cell Disease (Mucolipidosis 2). This disorder simulates Hurler syndrome with characteristic facies, marked skull and skeletal deformities with dwarfism (Fig. 9), joint contractures, and cardiac insufficiency. The diagnosis is made from elevation of betaglucuronidase and arylsulfatase A in white blood cells and of sialo-oligosaccharides in the urine.

Mucopolysaccharidoses

The disorders in this group are caused by deficiency of the various lysosomal enzymes involved in the degradation of glycosaminoglycans. The deficiency results in the storage of mucopolysaccharides in the cells of most organs, producing the typical gargoyle features. Skeletal involvement is reflected in dwarfism that, together with ligamentous thickening and weakening, may result in kyphosis and frequent vertebral subluxation, particularly at the atlantoaxial level (Fig. 10). Each or any combination of these changes may result in cord compression, which is a common cause of death in Morquio syndrome. Meningeal thickening may also be the cause of cord compression in the Hurler and Marateaux-Lamy syndromes, and result in hydrocephalus and arachnoid cyst formation in Hunter and Hurler diseases.

Macrocrania is a feature of mucopolysaccharidosis 1 and Hunter disease. It may be related to deposition of mucopolysaccharides in the Virchow-Robin spaces, resulting in varying degrees of distension. The individual spaces may be recognized deep in the white matter or in the basal ganglia (Fig. 11). They are usually most prominent in the parietal lobes as rounded or ovoid structures with their long axis extending across the white matter, causing density or signal

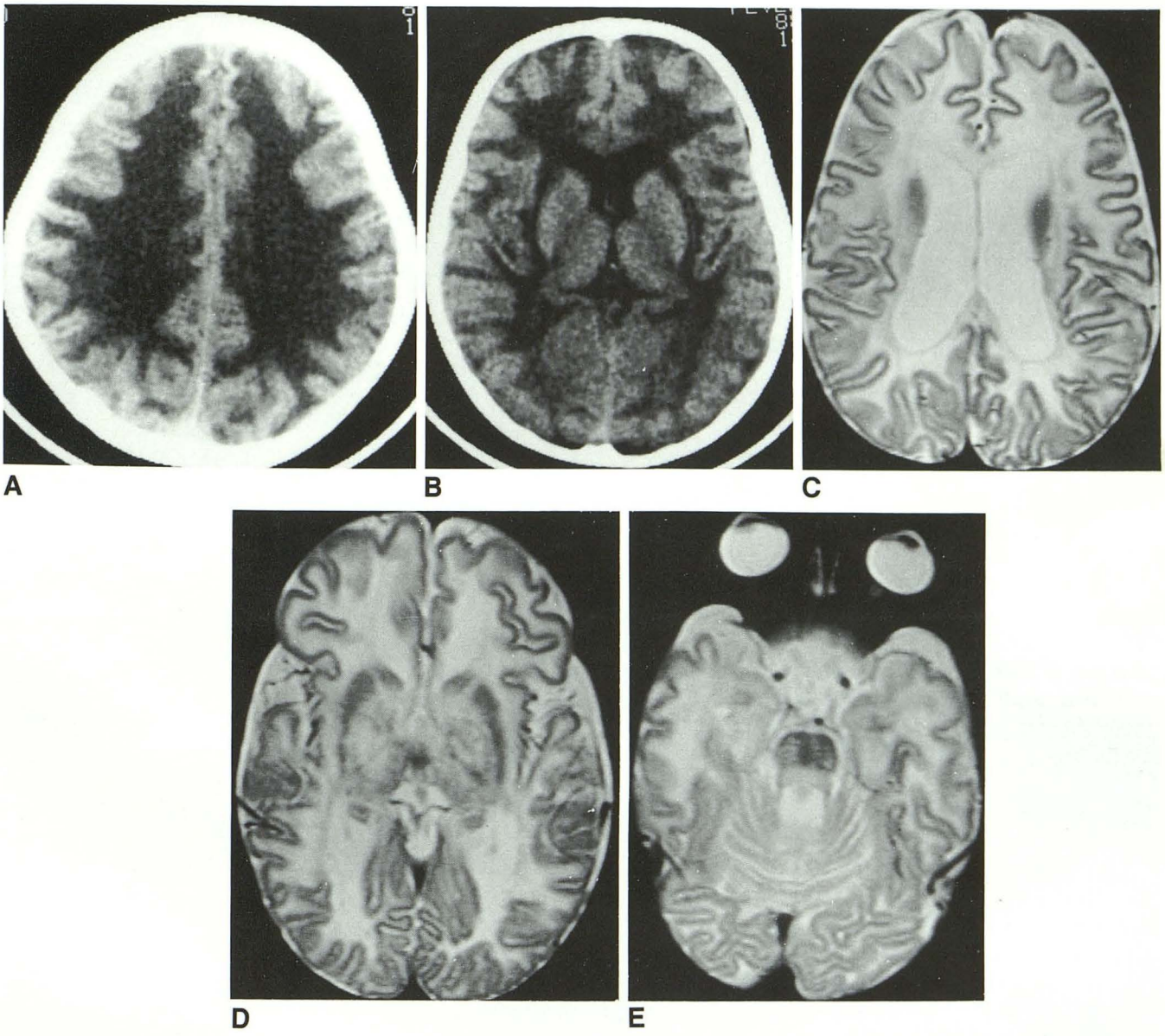

Fig. 7. Canavan disease; the child presented at age 2 years with macrocephaly and progressive loss of skills.

A and *B*, Axial CT. There is extensive symmetrical low density throughout the white matter of both hemispheres, extending into the gyral cores, and involving the external capsules.

C, *D*, and *E*, T2 MR at age 2 years, 8 months, after further clinical regression. There is limited myelination in the brain stem and internal capsules, abnormally high signal throughout the hemispheric white matter, and diffuse atrophy.

changes similar to CSF. Individual spaces may become very large or remain quite small; when multiple, the latter may cause a diffuse region of prolonged T1 and T2 values or of low CT density in the deep hemispheric white matter, simulating demyelination (Fig. 12).

Although the clinical diagnosis is generally obvious, CT and MR may be indicated where raised intracranial pressure is suspected, since complicating hydrocephalus and/or subdural effusion may be relieved by surgical treatment.

Multiple sulphatase deficiency combines the skeletal features of a mucopolysaccharidosis with the neurologic features of a leukodystrophy, and

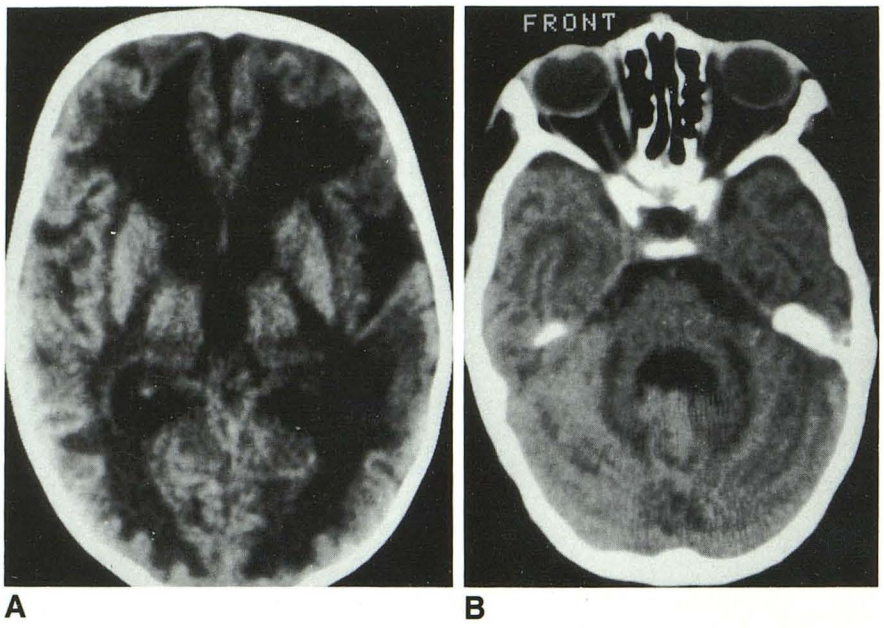

Fig. 8. Canavan disease; 4-year-old child with onset of progressive retardation, spasticity, and blindness during the second year. Axial CT sections through the internal capsules (*A*) and posterior fossa (*B*). There is symmetrical low density throughout the white matter of the cerebral hemispheres, the external and internal capsules, and the cerebellum. The ventricles and intracranial subarachnoid spaces are enlarged due to atrophy.

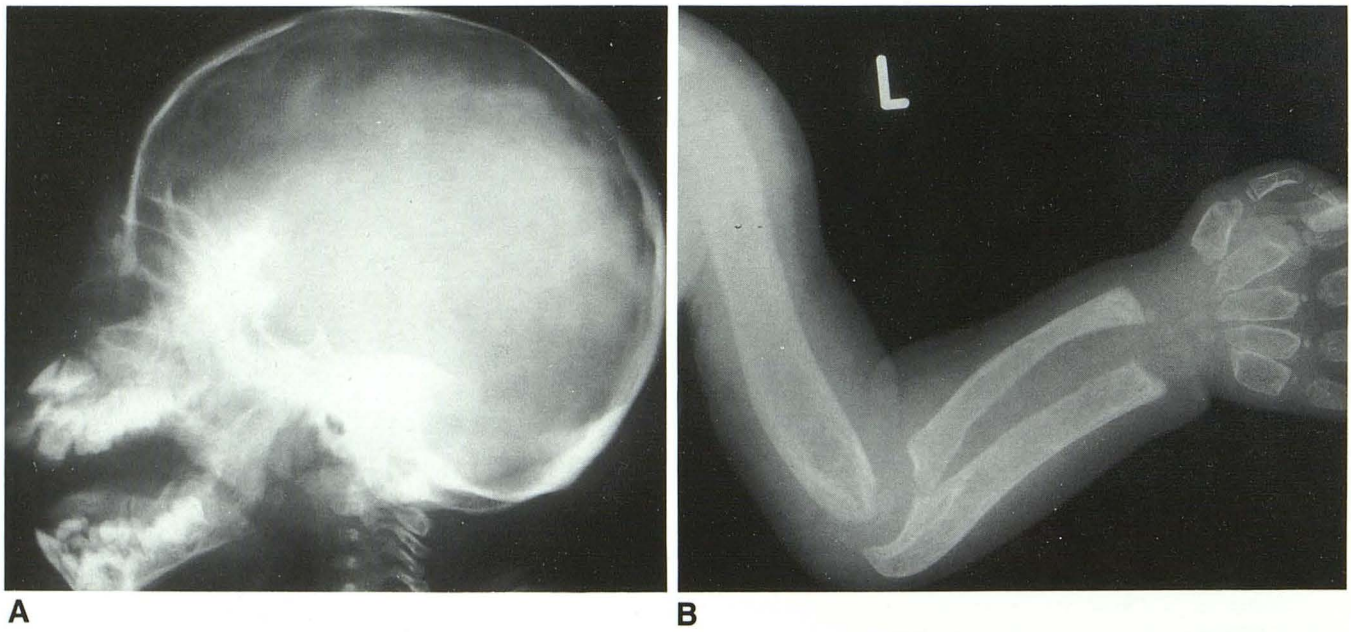

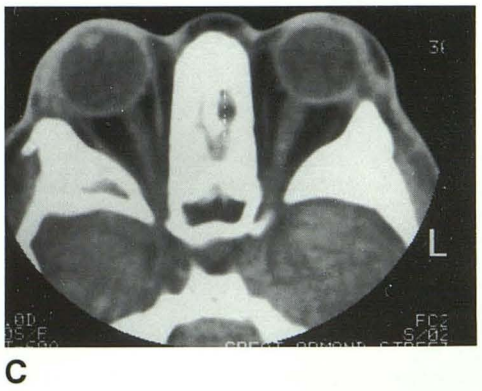

Fig. 9. I-Cell disease. *A*, Lateral skull radiograph; there is microcephaly with a large sella turcica. *B*, Axial CT; there is thickening of the bone, well shown in the lateral walls of the orbits. *C*, Left arm; the long bones are short, with abnormal thickening of the diaphysis, simulating Hurler disease.

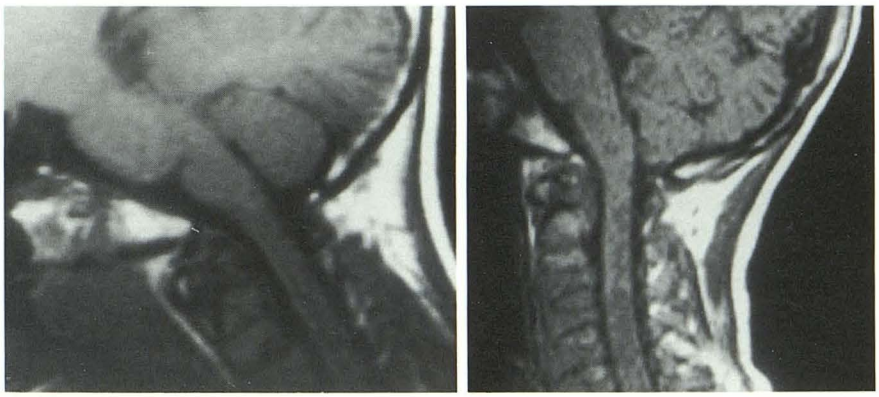

A B

Fig. 10. Morquio-Brailsford disease; 6-year-old boy with atlantoaxial subluxation on skull radiograph. Midsagittal T1 MR in flexion (*A*) and extension (*B*) shows mobile anterior atlantoaxial subluxation, an acquired os odontoideum, thickening of the retrodental tissues, and a minor degree of cord compression.

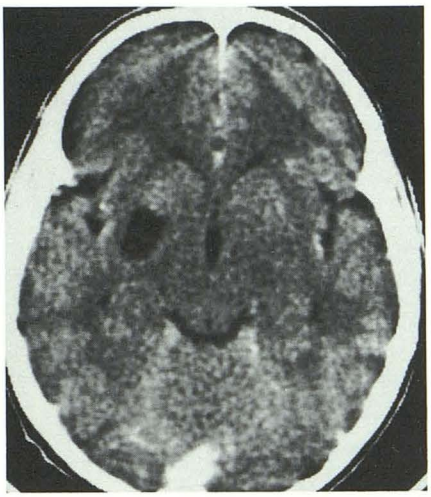

Fig. 11. Hunter disease; axial CT: there is a circumscribed, well-defined region of CSF density in the right lentiform nucleus, consistent with a distended Virchow-Robin space.

is associated with extensive density and signal changes in the cerebral white matter simulating metachromatic leukodystrophy.

Wolman Disease and Cholesterol Ester Storage Disease

These conditions are caused by deficiency of acid esterase, an enzyme essential to normal degradation of cholesterol esters and triglycerides by hydrolysis of ester bonds.

In Wolman disease, the esters are stored in reticuloendothelial cells and phagocytes within the stroma of most organs, and are recognized as sudanophyllic inclusions within the liposomes. The diagnosis can be suspected from inclusions in the white blood cells and confirmed by a deficiency of acid esterase in the leukocytes or in cultured skin fibroblasts.

The disease is usually manifest within weeks of birth, presenting with hepatosplenomegaly, adrenal enlargement and calcification, and gastrointestinal upset followed by regression, paresis, and spasticity. The children become cachectic and usually die before 6 months. Cholesterol ester storage disease may run a much less drastic course and may even occur in adulthood.

In the brain, sudanophilic lipid is stored in microglia, leptomeninges, and choroid plexuses. Demyelination and gliosis are variable in degree. The disease is one cause of sudanophilic leukodystrophy and is indistinguishable from other sudanophylic leukodystrophies on computed imaging.

Pompe Disease

This condition is associated with deficiency of the enzyme maltase and results in intraliposomal deposition of glycogen in all cells and also interstitially. Deposition within muscles results in myopathy, clinically evident swelling of the tongue, and cardiac enlargement. Heart failure usually leads to death within 2 years. Deposition within neurones and astrocytes in the brain and spinal cord is associated with gliosis.

Ceroid Lipofuscinoses

The basic defects in this autosomal recessively inherited group of conditions and the precise composition of the materials stored in the neural and visceral cells are not known. However, recent research has allowed reclassification of the disease into two groups based on whether the pro-

tein component, sub-unit C of mitochondrial adenosine triphosphate (ATP) synthesase, is present or absent in the stored lipopigment. The protein component is seen in the late infantile, juvenile, and in most cases of the adult Kufs disease. The protein component is absent and granular osmiophilic deposits are present in the second group that includes the infantile and some juvenile and adult cases.

On computed imaging, cerebral and more prominent cerebellar atrophy (Fig. 13) are usual (9). Low density on CT has been shown in the hemispheric white matter in the infantile type (10). Hyperintense periventricular white matter has been noted on T2-weighted MR in advanced infantile and juvenile ceroid lipofuscinoses (11). The disease causes epilepsy, associated with myoclonus, mental retardation, ataxia, and loss of vision. The diagnosis is usually confirmed by typical electroencephalographic and evoked potential abnormalities. However, these may occur late in some variants. CT and MR may then provide some collaborative evidence for the diagnosis.

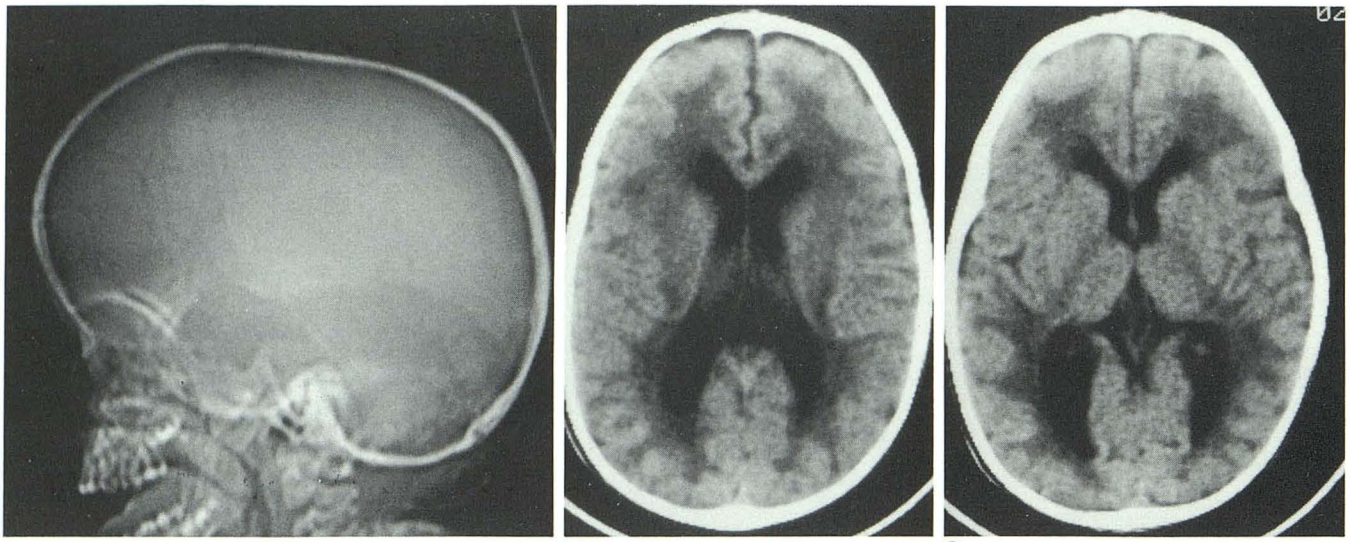

Fig. 12. Hurler disease with macrocrania.

A, Cranial CT; Scout view shows macrocrania.

B and *C*, Axial CT sections through the corona radiata (*B*) and internal capsule (*C*). There is extensive inhomogeneous low density in the deep white matter. The lateral ventricles are slightly enlarged, but the third ventricle is of normal size.

Fig. 13. Ceroid lipofuscinosis; onset at age 12 years with increasing dementia, visual failure, ataxia, and mycoclinic jerks.

A, Midsagittal T1 MR shows gross cerebellar atrophy with mild brain stem and cerebral atrophy.

B, Axial T2 MR shows diminished signal in the deep gray matter, and slightly increased signal in the parietal white matter.

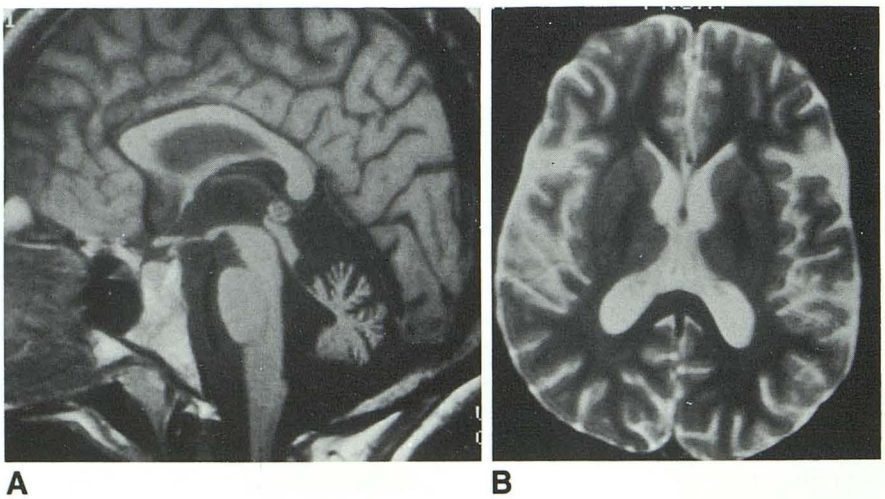

Peroxisomal disorders

Peroxisomes are intracellular organelles, 0.15–1.5 μm in diameter, that consist of a single layered membrane enclosing a matrix. They contain respiratory enzymes in both the matrix and the membrane. Light and electron microscopy shows peroxisomes are present in most cells. Their enzymes are known to be involved in several functions.

1. They are vital for the oxidation of very long-chain (~24–26) and monounsaturated fatty acids.
2. They take part in the beta-oxidation of dicarboxylic acids, the oxidation of the exogenous metabolite phytanic acid, the catabolism of glutaric acid, the metabolism of lysine, and the transamination of amino acids in gluconeogenesis.
3. They take part in the synthesis of bile acids and ether phospholipids. The latter include plasmalogens, which are constituents of myelin, and many cell membranes and alkylglycerophospholipids, including platelet-activating factor, which is important in various inflammatory processes.

Peroxisomal disorders form the basis of several inherited metabolic defects and a group of syndromes characterized by absence or varying degrees of deficient function of one or more of these enzymes (12). In most of these conditions, the central and/or peripheral nervous system is involved.

The central nervous system abnormalities include:

1. Disturbances of neuronal migration, usually accompanied by dysmyelination, delayed myelination, or demyelination, found in the cerebrohepatorenal syndrome of Zellweger, neonatal adrenoleukodystrophy, and pseudo-Zellweger syndrome.
2. Symmetrical dysmyelination or demyelination often of characteristic distribution.
3. Cranial and peripheral neuropathies.

In some of the peroxisomal disorders, the diagnosis can be suspected clinically, but, in others, the presentation is far from specific. The diagnosis is confirmed biochemically.

In many of the diseases, the appearances on computed imaging are more or less specific and may precede any clinical abnormalities. In others, they are much less specific and may only become evident when clinical abnormalities have been present for several years.

The diseases are classified into two groups, depending on whether there is reduced activity of a single enzyme or the deficiency is multiple.

Single Enzyme Deficiencies

Adrenoleukodystrophy. The most common condition of the first group is X-linked adrenoleukodystrophy (ALD) caused by a deficiency of acyl-CoA synthesase. The deficiency prevents effective breakdown of very long-chain fatty acids, so these are incorporated in cholesterol esters to the exclusion of nonesterified cholesterol. Symptoms are usually evident in affected boys between the ages of 5 and 7 years. The neurologic deficits may be preceded by adrenal insufficiency and be precipitated by an intercurrent infection. The commonest are regression and behavior disturbances, associated with disorders of vision and hearing. Symmetrical alteration in white matter is usually first evident in the peritrigonal regions and extending through the splenium of the corpus callosum. Though characteristic, this distribution has also been recorded in other conditions such as late juvenile onset Krabbe disease (13). The abnormality extends circumferentially to involve the occipital lobes and more anterior regions of the hemispheres. The medial and lateral geniculate bodies and the adjacent thalami and the superior and inferior brachia are generally involved. There are alterations in the pyramidal tracts and in the occipito-temporo-parieto-pontine fibers, with sparing of the frontopontine fibers in the medial part of the crus cerebri (Fig. 14). The lateral lemnisci and the cerebellar white matter may be involved. Atypical cases are recorded in which the disease commenced by involving the white matter of other lobes, or was asymmetrical or even unilateral (14).

The affected cerebral white matter typically consists of three zones (Fig. 15):

1. A central zone in which the myelin has been replaced by a mesh of glial fibers. Sometimes there is necrosis with cavitation or calcification in this region (Fig. 16).
2. An intermediate zone in which demyelination is associated with active inflammatory changes. This zone enhances with intravenous contrast agents.
3. A peripheral zone of demyelination without inflammatory reaction.

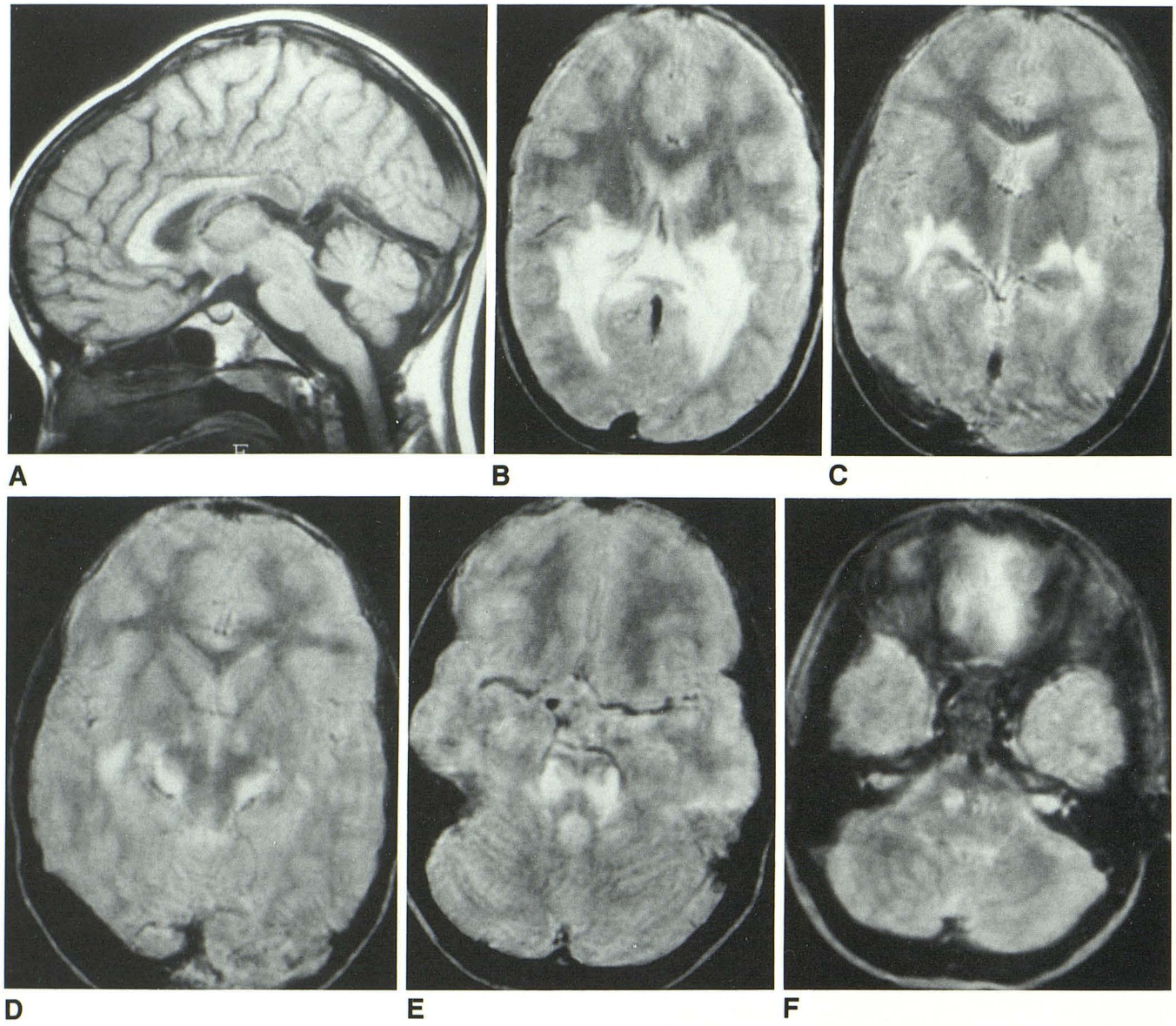

Fig. 14. Adrenoleukodystrophy.

A, Sagittal T1 MR shows low signal in the splenium.

B–F, Serial axial T2 MR. There is high signal within the peritrigonal white matter, the splenium of the corpus callosum, the superior and inferior brachia and geniculate bodies and adjacent parts of the thalami, the lateral lemnisci (*E*), and the pyramidal tracts sparing the frontopontine fibers in the medial third of the crus (*E*).

The whole abnormal region is low in density on plain CT, but the intermediate enhancing zone is usually evident as a band on relatively higher density. The lesion reflects high signal on T2- and low signal on T1-weighted MR sequences, the signal change being more prominent from the peripheral zone. In advanced cases, atrophy is usual and low density may become less marked, leaving atrophy as the dominant feature (Fig. 16).

X-linked adrenomyeloneuropathy (AMN) is caused by a similar enzyme defect: it frequently occurs in the same family as ALD but presents later in life. Demyelination is most marked in the corticospinal and spinocerebellar tracts, but it does extend through the brain stem, involving the pyramidal tracts, and up through the posterior limb of the internal capsule (Fig. 17). The frontopontine as well as the occipito-temporo-parieto-pontine fibers are affected, so that signal change is present across the whole width of the crus

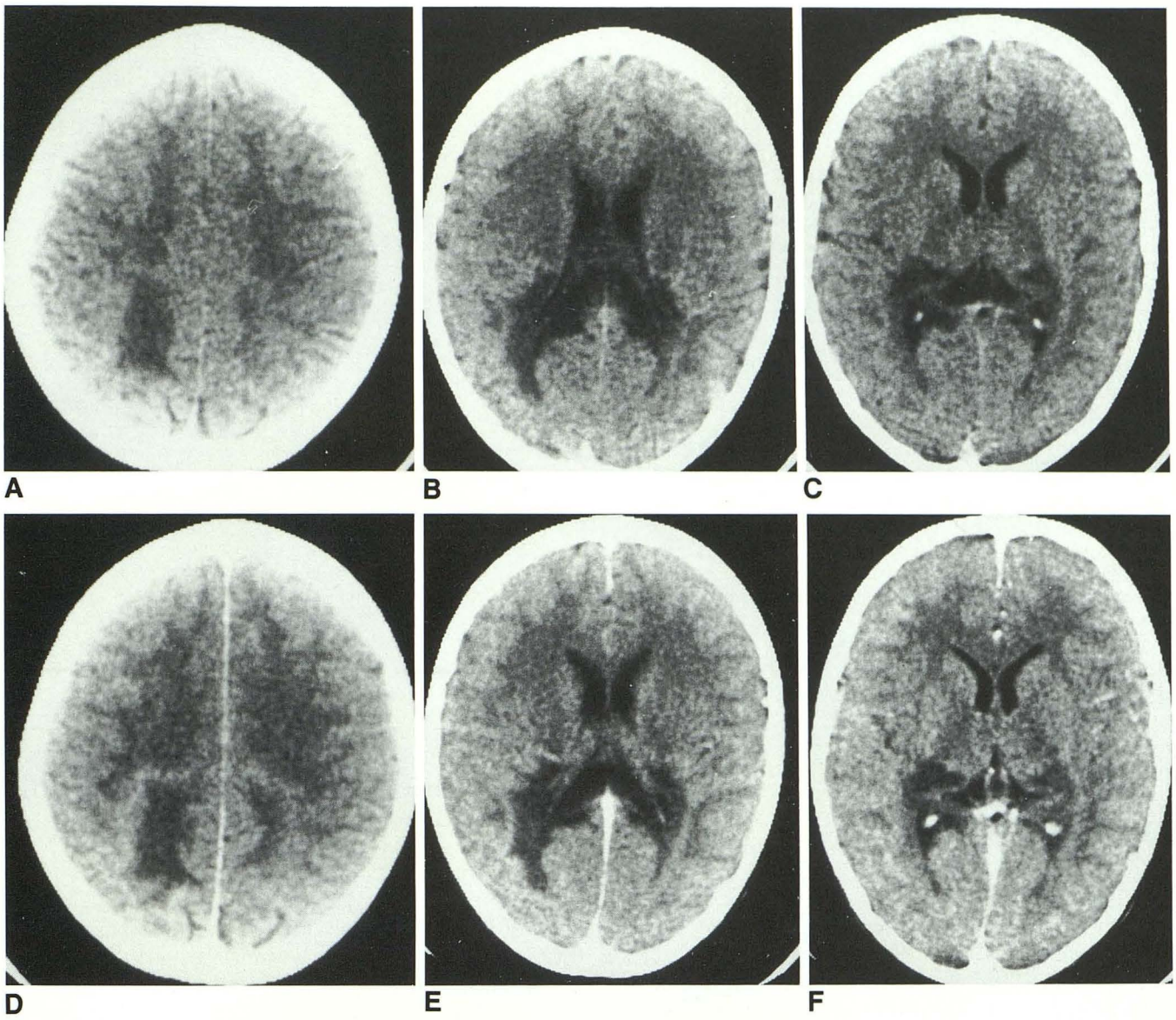

Fig. 15. Adrenoleukodystrophy; cranial CT: before (*A–C*) and after (*D–F*) intravenous contrast administration. The lesion shows the typical three zones, with enhancement of the intermediate high-density zone, most evident in *D* and *E*. The disease involves the peritrigonal and medial parietal white matter, the splenium of the corpus callosum, the lateral geniculate bodies, and posterior parts of the thalami.

cerebri. This region may be continuous with the involved medial lemniscus (15). The cerebellar white matter is also affected, but the cerebral white matter is usually spared. The disease is often far advanced before MR becomes abnormal.

In symptomatic female carriers of X-linked ALD, the course of the disease is usually benign and tends to simulate AMN. Computed imaging may be normal or show changes similar to either AMN or ALD.

Pseudoneonatal ALD

In pseudoneonatal ALD, the enzyme deficiency is confined to fatty acyl-CoA oxidase. Progressive neurologic deficit occurs early in life. CT, which is said to be normal at first, shows progressive white matter changes and abnormal contrast enhancement, which become extensive (16). MR has been described in a single case in which multiple studies from the age of 1 month to 3

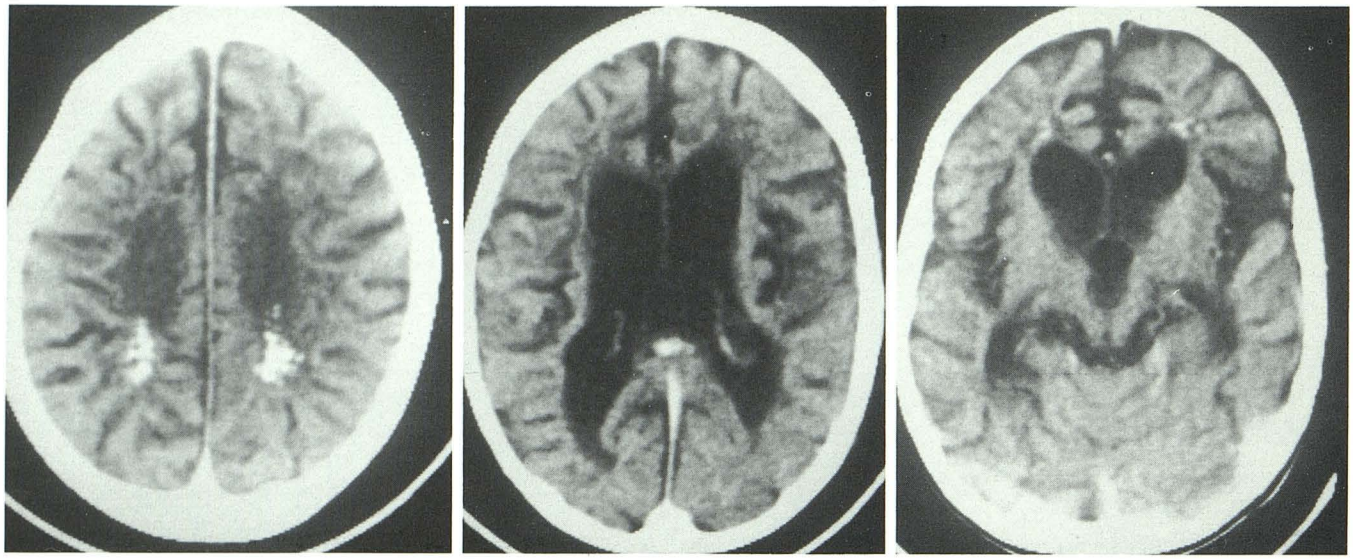

Fig. 16. Adrenoleukodystrophy. Axial CT sections above the lateral ventricles (*A*), through the bodies of the lateral ventricles (*B*), and through the third ventricle (*C*). There is diffuse cerebral atrophy, a thin rim of low density in the periventricular white matter, and patchy calcification within the white matter adjacent to the superior borders of the trigones and frontal horns.

years showed delayed myelination followed by symmetrical demyelination of the corona radiata, optic radiations, and pyramidal tracts (15).

Refsum Disease

In Refsum disease, deficiency of phytanic acid 2-hydroxylase prevents metabolism of exogenous phytanic acid, which is incorporated into myelin. This incorporation is greater in the peripheral than in the CNS, because the peripheral nervous system has more rapid turnover of myelin. The abnormal myelin has diminished viability, so that demyelination occurs in peripheral nerves and in the CNS. This typically produces a peripheral and cranial neuropathy, but central involvement may be manifest with demyelination of ascending and descending tracts in the spinal cord, brain stem, cerebellum, and central white matter. In less severely affected patients, computed imaging is normal, but the abnormal white matter may show symmetrical low density on CT (Fig. 18) and high signal on T2-weighted MR. The affected nerves are enlarged and should be demonstrable on CT and MR, as in other hypertrophic neuropathies on CT and MR.

Skeletal manifestations may suggest the diagnosis in appropriate clinical context. They include epiphyseal dysplasia and abnormal shortening or elongation of the second metatarsal.

Cerebrotendinous Xanthomatosis

This rare autosomal recessive disorder is associated with abnormal peroxisomes, but there is evidence that mitochondria may be abnormal also. The basic defect is uncertain, but 26 hydroxylase and 24S hydroxylase deficiencies have been suggested. Impaired cleavage of cholesterol side chain leads to defective conversion of cholesterol to bile acids with accumulation of cholestanol, either free or within macrophages. The abnormal lipid accumulates in tendons, within the choroid plexuses, and within perivascular spaces of the CNS, particularly within the cerebellum. There is microglial reaction and fibrillary gliosis. Cholestanol may also be incorporated within myelin membranes, rendering them unstable and possibly accounting for demyelination. This affects particularly the cerebellum and its connections, but also involves the dorsal columns, pyramidal tracts, and the transverse pontine fibers.

The patients are generally of low intelligence and show progressive retardation. Cerebellar ataxia, epilepsy, and pseudobulbar palsy are slowly progressive, but death does not usually occur until late middle age. Calcification may be seen in deposits in the tendons, adrenal glands, and coronary arteries.

CT may show low density in affected cerebellar and, less often, in cerebral white matter (17). In

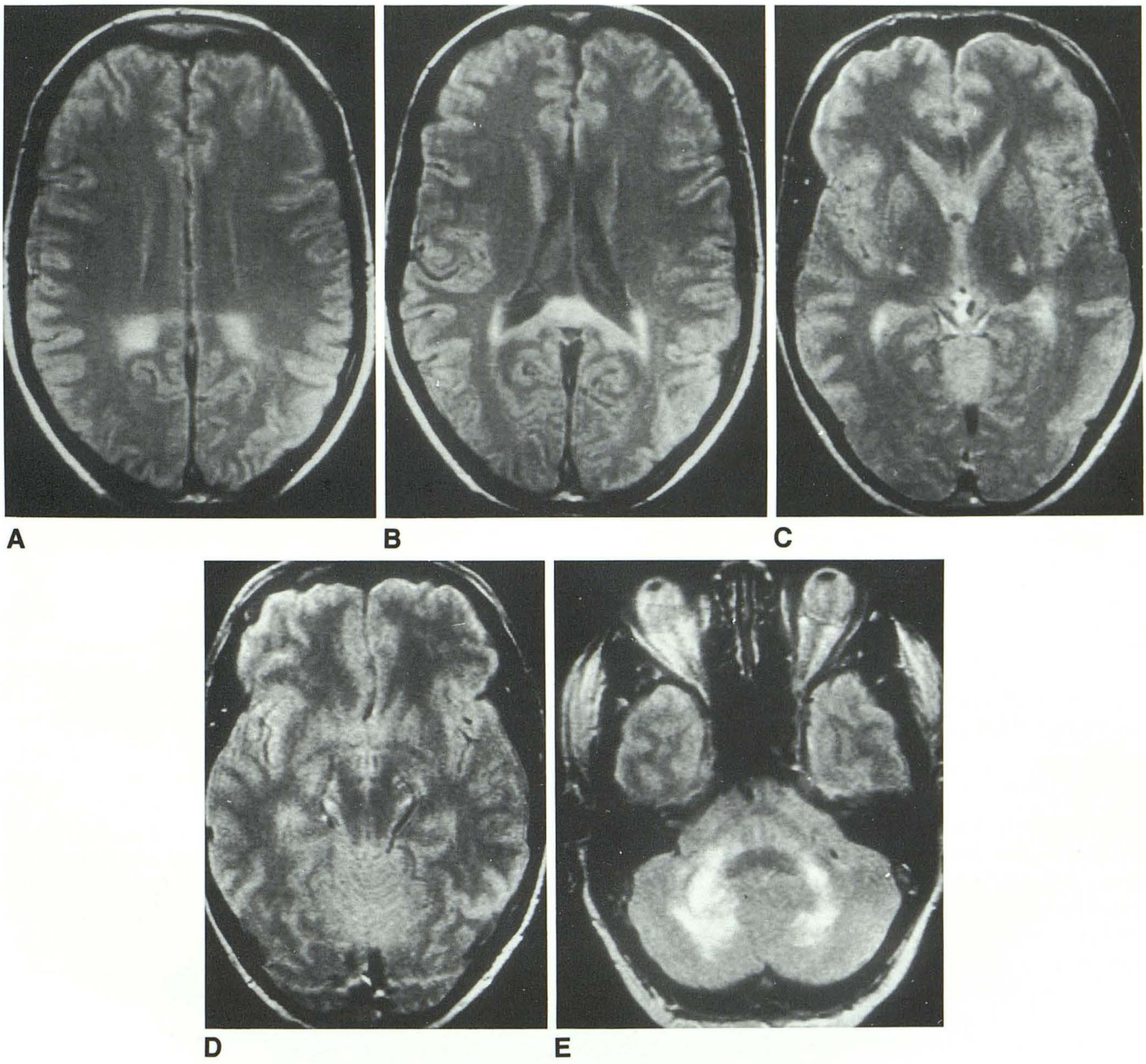

Fig. 17. Adrenomyeloneuropathy; *A–E*, Axial T2 MR sections. High signal involves the peritrigonal white matter, the splenium of the corpus callosum, the pyramidal tracts, the crus cerebri, the medial lemniscus, and the cerebellar white matter.

our single example, MR (Fig. 19) showed more extensive, but equally nonspecific, changes.

Abetalipoproteinaemia

This autosomal recessive condition is probably due to a peroxisomal enzyme defect, although this is not proven. There is failure of synthesis of apolipoprotein, which is essential for the construction of low-density lipoproteins and chylomicrons. This leads to alteration in the walls of red blood cells, causing acanthocytosis, and in myelin membranes, causing demyelination.

Demyelination is most pronounced in the dorsal columns, spinocerebellar tracts, and the cerebellar white matter. The pyramidal tracts are involved to a lesser degree. The anterior horn cells of the spinal cord degenerate.

Intestinal malabsorption is associated with growth failure; neurologic symptoms usually

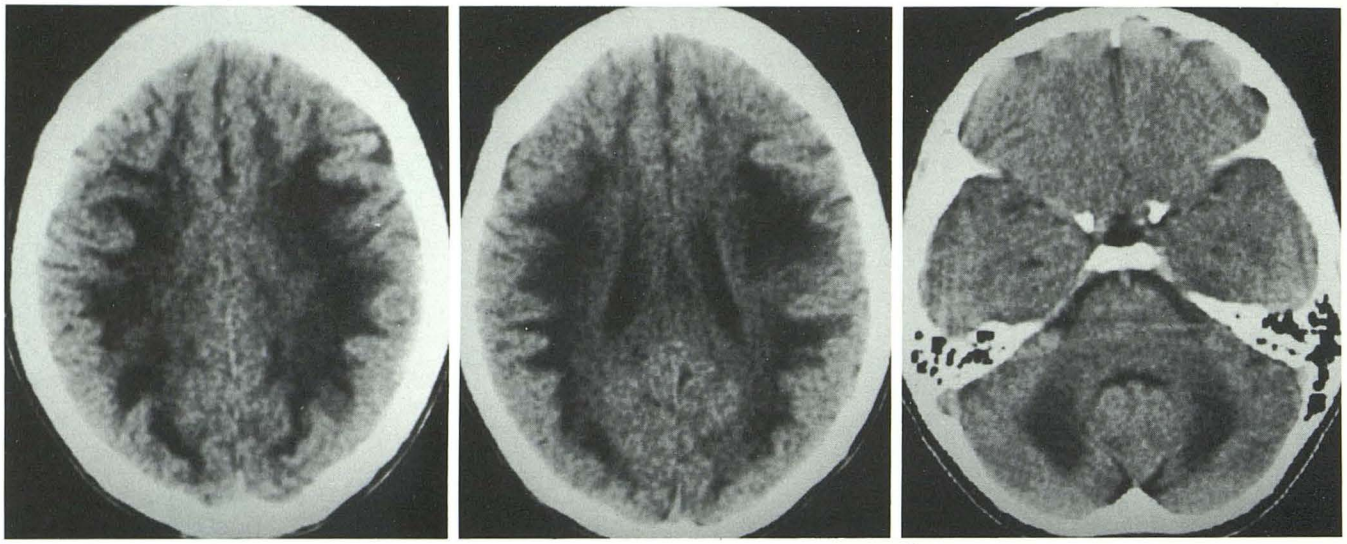

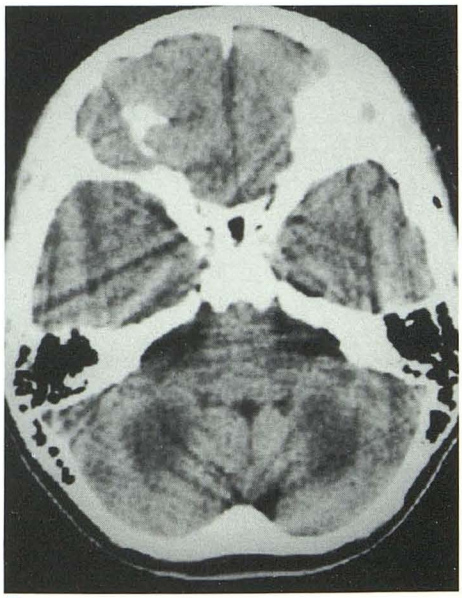

Fig. 18. Refsum disease. Axial CT sections through supraventricular white matter (*A*), lateral ventricles (*B*), pons (*C*), and medulla (*D*). There is extensive symmetrical low density in the cerebellar and cerebral white matter.

commence at about the age of 5 years and include ataxia and weakness, and pigmentary degeneration of the retina causing blindness. Sensory and cerebellar ataxia have a slowly progressive course.

Computed imaging shows marked cerebellar atrophy and symmetrical, nonspecific changes in the cerebellar and cerebral white matter.

Conditions Associated with Deficiency of Multiple Peroxisomal Enzymes

Cerebrohepatorenal Syndrome of Zellweger. This autosomal recessive condition causes liver dysfunction with jaundice, marked mental retardation, weakness, and hypotonia. It may progress to death in early childhood. The amount of peroxisomal activity determines disease severity in each individual. Ultrasonic examination of the kidneys reveals small cortical cysts. Radiographic examination of the limbs reveals abnormal calcification in the patella, greater trochanter, and triradiate cartilages in 50%–75% of patients.

Cerebral abnormality, better shown by MR than CT, consists of:

1. Disturbed neuronal migration with a thickened cortex and diminished volume of white matter, resulting in focal pachygyria, polymicrogyria, and periventricular and intracerebral cortical heterotopia.

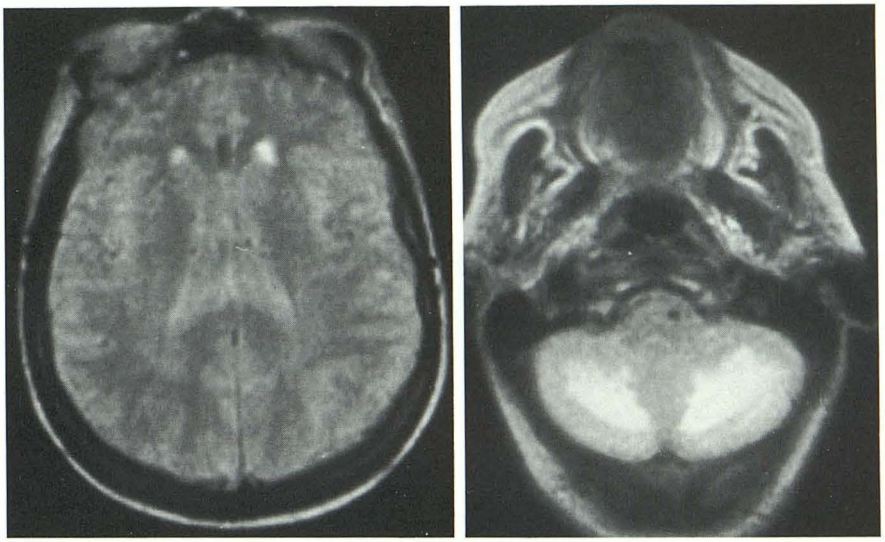

Fig. 19. Cerebrotendinous xanthomatosis; 45-year-old woman. Axial T2 MR sections through the lateral ventricles (*A*) and cerebellum (*B*). The high signal adjacent to the frontal horns is prominent and probably abnormal; otherwise, the cerebral white matter is normal. There is abnormal high signal throughout the white matter of both cerebellar hemispheres.

2. Abnormal myelin with delay in myelination and possible demyelination with gliosis.

Neonatal Adrenoleukodystrophy

In addition to the typical enzyme deficiencies of X-linked ALD, there is pipecolic and phytanic acidemia and deficiency of plasmalogen synthesis. The disease is inherited as an autosomal recessive.

In common with Zellweger syndrome, there are general defects of neuronal migration with pachygyria, polymicrogyria, and heterotopic gray matter. There is also diffuse demyelination affecting both cerebral and cerebellar hemispheres, with demyelination of descending tracts in the brain stem. The diffuse demyelination excites an inflammatory cellular response that produces enhancement in the lesions on computed images.

Infantile Refsum Disease

In addition to phytanic acidemia, there are more generalized deficiencies of peroxisomal enzymes. This disease presents early in life and involves both sexes equally, suggesting an autosomal recessive form of inheritance. Cranial and peripheral neuropathies are associated with retinitis pigmentosa and mental retardation. There is no evidence of neuronal migration defect. Cranial and computed imaging may be normal. However, diminished myelination with gliosis has been shown at autopsy and, in two children examined by us, there was low density in the parietal white matter on CT, with high signal from the same region and from the posterior limbs of the internal capsules and pyramidal tracts (Fig. 20) on MR. There was no abnormal enhancement.

Hyperpipecolic Acidemia

This is an extremely rare autosomal recessive condition in which, at autopsy, both absent myelination and demyelination of white matter without inflammatory response have been described.

Rhizomelic Chondrodysplasia Calcificans Punctata

In addition to the limb changes that are evident on plain radiographs, there is marked delay in myelination and sometimes demyelination. MR has shown abnormal signal in the periventricular and subcortical white matter, particularly in the posterior parts of the hemispheres, with progressive atrophy (18).

Mitochondrial Disorders

Mitochondria are cytoplasmic thread-like structures up to 1 μm in diameter and of variable length. They contain the DNA coding for production of numerous polypeptide enzymes involved in the respiratory chain (19). These enzymes are necessary for the formation of ATP that fuels the high energy requirements of cellular metabolism. They control the Krebs cycle and include also:

1. The pyruvate dehydrogenase complex in-

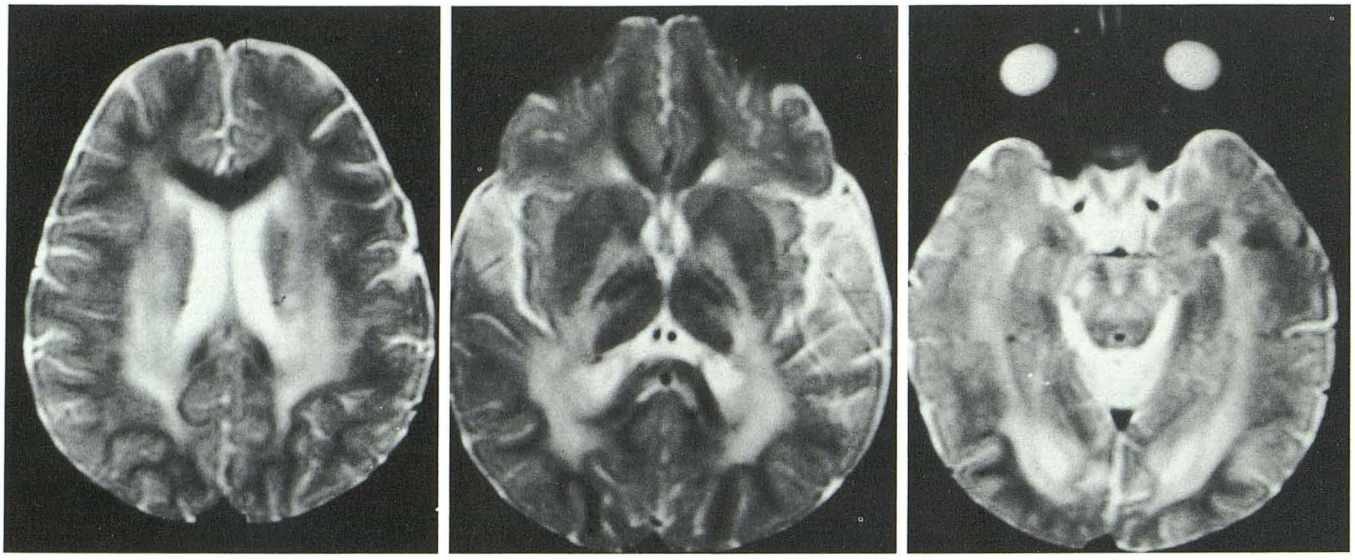

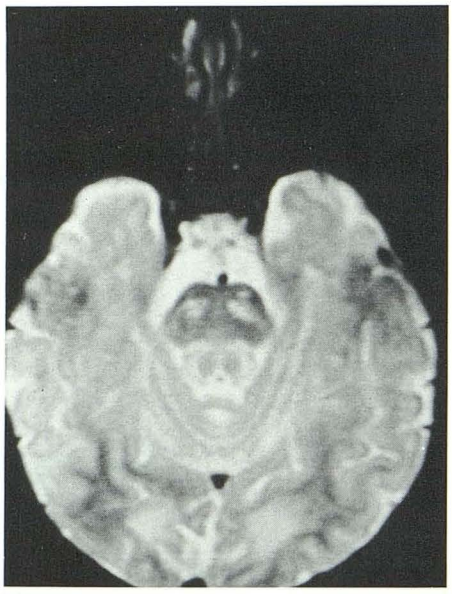

Fig. 20. Infantile Refsum disease; 2-year-old girl. T2 MR sections (1.5 T) at level of the lateral ventricles (*A*), third ventricle (*B*) midbrain (*C*), and pons (*D*). There is symmetrical high signal in the deep white matter of the parietal occipital and posterior temporal lobes, involving the posterior limbs and genus of the internal capsules and the pyramidal fibers in the crura and pons.

volved in oxidative decarboxylation of pyruvate derived from glucose and glycogen; and

2. carnitine palmityl transferases that facilitate the conversion of free fatty acids to acetyl CoA. The acetyl-CoA thus produced enters the Krebs cycle for oxidation to carbon dioxide with release of the hydrogen utilized by respiratory enzymes to form ATP.

Mitochondrial Cytopathies

The mitochondrial cytopathies form a characteristic group of mitochondrial dysfunctions, which are transmitted by non-Mendelian maternal inheritance. They have been classified on a biochemical basis (20). This classification does not specifically correlate with particular clinical abnormalities that may vary considerably within a single kindred (21). These include myopathic weakness and fatiguability of muscles, particularly those of the limb girdles, ophthalmoplegia, peripheral neuropathy, and symmetrical or asymmetrical CNS deficits.

Many other organs may be affected including:

1. endocrine glands causing growth hormone deficit with dwarfism, hypoparathyroidism, and hypothyroidism;

2. the hemopoietic system, causing normochromic anaemia;
3. the myocardium, causing heart block and/or cardiomyopathy;
4. the eyes, resulting in pigmentary retinopathy; and
5. the liver, resulting in abnormal function tests.

Morphologic changes shown on computed imaging may strongly suggest this group of disorders but are not generally specific for a particular enzyme defect.

The impaired aerobic metabolism of pyruvate (Fig. 21) results in anaerobic conversion to lactate and transamination to alanine. All three substances may be detected in the serum. Lactate may be shown by spectroscopy within the brain lesions. Though nonspecific, this may be helpful in the further study of these disorders.

Subacute Necrotizing Encephalomyelopathy (Leigh Syndrome). Young children are preferentially affected, but older children and adults may be involved. The onset may be acute, remitting or slowly progressive with ophthalmoplegia, extrapyramidal and/or cerebellar signs, spasticity, or bulbar palsy. Spongy degeneration is associated with astro- and microglial reaction and vascular proliferation affecting the basal ganglia, brain stem, and spinal cord. Early involvement of the cerebral cortex also occurs. There may be demyelination of cerebral and cerebellar white matter, with preservation of nerve cells and axons. These lesions are associated with low density on CT and signal change on MR; hyperechoic changes may allow early recognition of lesions in infants at risk using ultrasound (22). The globus pallidus, thalamic and subthalamic nuclei in children, and the brain stem in adults are most characteristically affected (Fig. 22). There may be swelling in the acute phase but resolution may be remarkable, leaving only slight residual lesions resembling small foci of necrosis or lacunes (Fig. 23).

MELAS (Mitochondrial encephalomyelopathy, lactic acidosis, and stroke-like episodes). Stroke-like episodes cause acute focal neurologic deficits and/or seizures. Infarction may be simulated, affecting any part of the brain substance, but the posterior parts of the hemispheres are more commonly affected on CT (23) and MR (Fig. 24) (24). The blood vessels do not appear significantly abnormal on angiograms (25). The acute lesions consist of encephalomalacia associated with gliosis and vascular proliferation. Acute lesions may resolve within a month (26, 27), although there may be residual focal or more generalized atrophy. More chronic lesions may be present in the basal ganglia associated with more or less symmetrical necrosis or calcification (Fig. 24) (28).

MERRF (Myoclonic epilepsy with ragged red fibers). In addition to myoclonic epilepsy and muscle weakness, as in MELAS, there may be more generalized features of a mitochondrial cytopathy, including short stature, cardiac conduction defects, and endocrine deficiencies. There

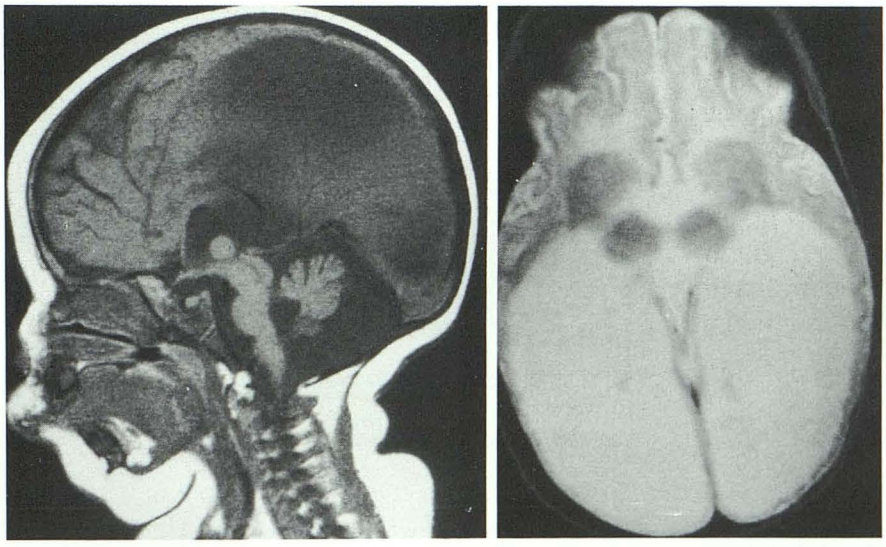

Fig. 21. Pyruvic dehydrogenase deficiency; 5-month-old child with failure to thrive, hypotonia, and increased lactic acid in blood and CSF. Midsagittal T1 MR (*A*) and axial T2 MR (*B*) at the level of the thalami. There is gross cerebral and less marked cerebellar atrophy with very small thalami.

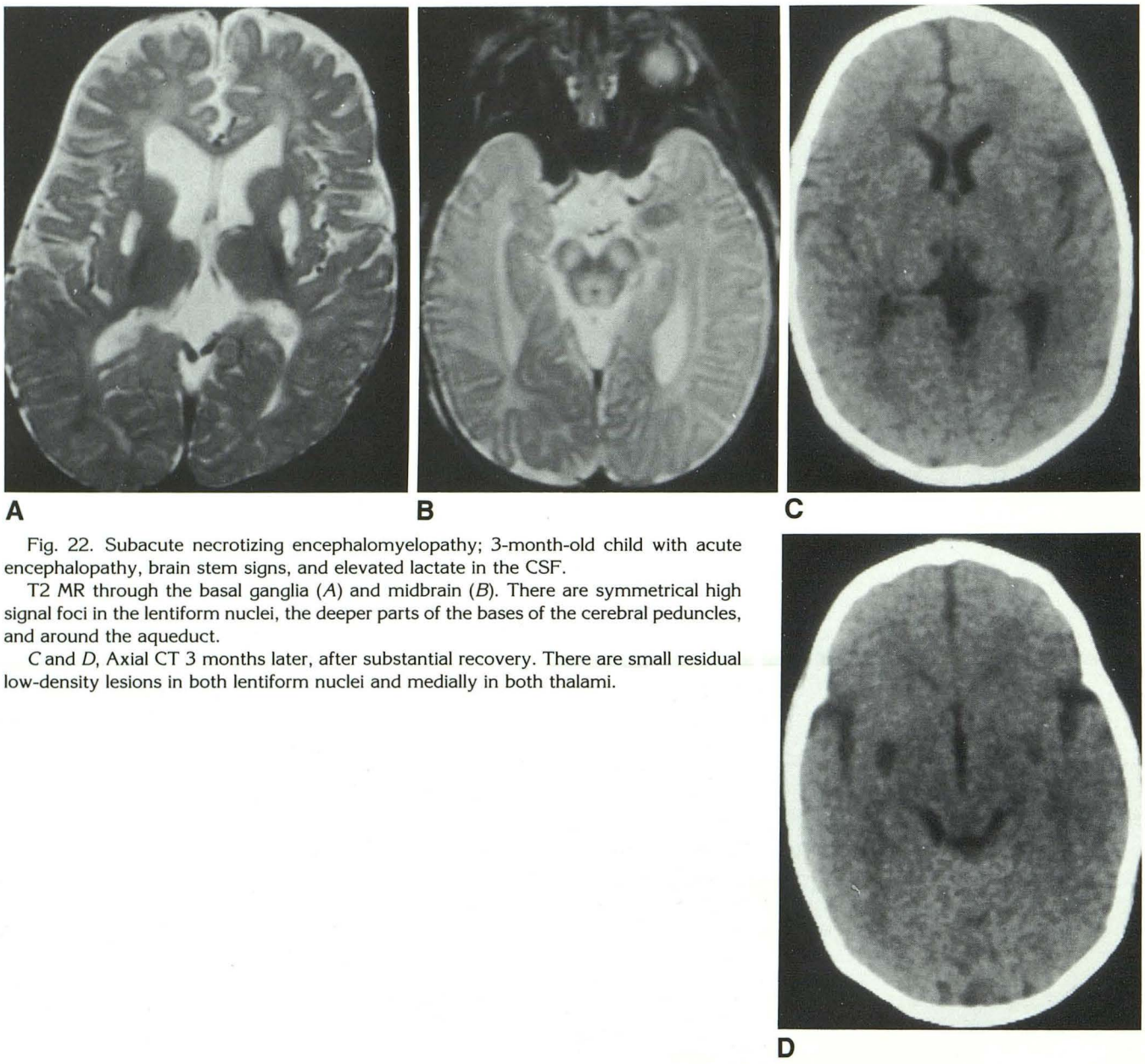

Fig. 22. Subacute necrotizing encephalomyelopathy; 3-month-old child with acute encephalopathy, brain stem signs, and elevated lactate in the CSF.

T2 MR through the basal ganglia (*A*) and midbrain (*B*). There are symmetrical high signal foci in the lentiform nuclei, the deeper parts of the bases of the cerebral peduncles, and around the aqueduct.

C and *D*, Axial CT 3 months later, after substantial recovery. There are small residual low-density lesions in both lentiform nuclei and medially in both thalami.

may be spongiform degeneration of cerebral and/or cerebellar white matter with low density on CT (Fig. 25) and signal changes on MR. Cerebral and cerebellar atrophy are frequent, but about half the proven cases have shown no abnormality on neuroimaging.

Kearns-Sayre Syndrome. Kearns-Sayre syndrome consists of chronic progressive external ophthalmoplegia, pigmentary degeneration of the retina, heart block, and limb weakness. Not all these features are consistently present; additional features that overlap MELAS and MERRF may be associated (29). Computed imaging may show iron deposition and calcification in the basal ganglia, with cerebellar and midbrain atrophy (Fig. 26). Additionally, there may be spongiform degeneration of cerebral and cerebellar white matter, sometimes also involving the basal ganglia, thalami, dentate nuclei, brain stem, and cervical spinal cord, with appropriate signal changes on MR (30).

Poliodystrophy (Alpers Disease)

This condition may be associated with deficiency of cytochrome *c*-oxidase (31) or hepatic pyruvate co-carboxylase (32). It usually occurs in

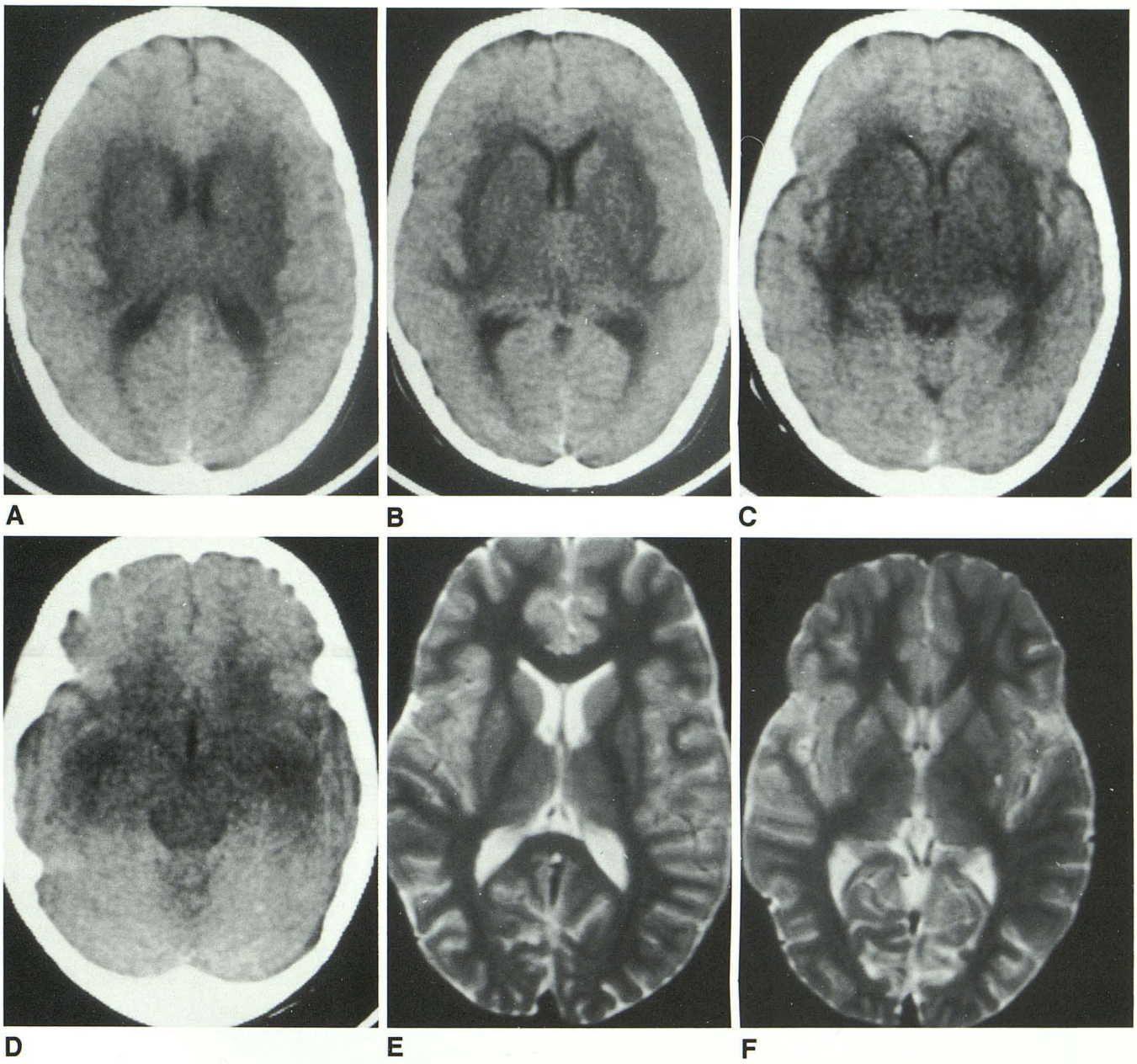

Fig. 23. Leigh syndrome with lactic acidosis.

A–D, Axial CT sections. There is extensive low density involving most of the deep gray matter, the deep hemispheric white matter and the brain stem, and focal brain swelling.

E and *F*, T2 MR sections, 3 months later following recovery from the acute phase. Apart from small foci of high signal in the lentiform nuclei, the lesions appear to have resolved. CT was normal at this stage.

early infancy, although occasionally it is milder with a later onset. It causes refractory convulsions, mental retardation, and spasticity, progressing to decerebration and microcephaly. Spongy degeneration affects the cerebral cortex, particularly the posterior parts, but also the deep gray matter and brain stem with astrocytic reaction. Iron and calcium may be deposited in the basal ganglia. Computed imaging may reveal focal lesions of white and gray matter that are

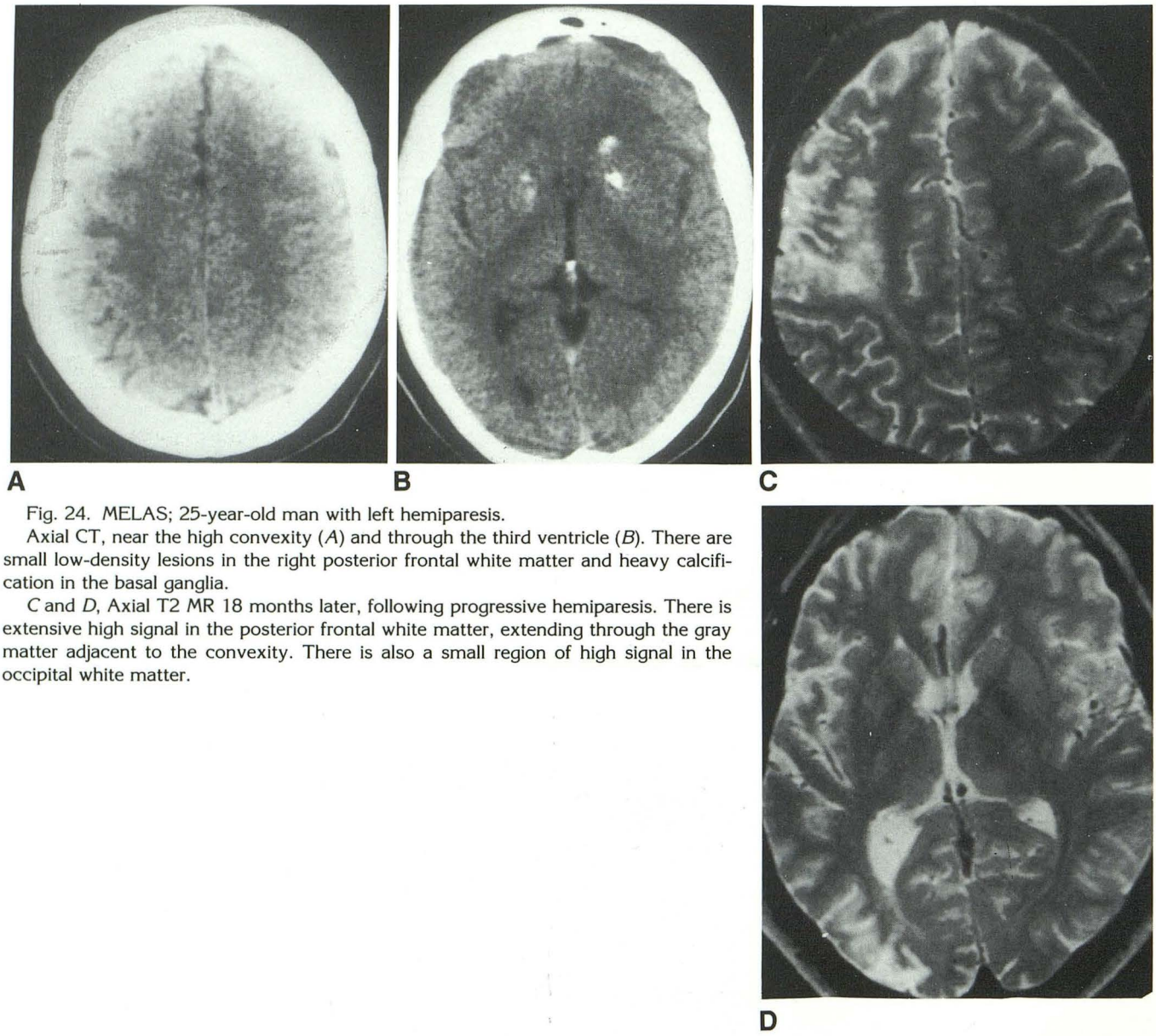

Fig. 24. MELAS; 25-year-old man with left hemiparesis.

Axial CT, near the high convexity (*A*) and through the third ventricle (*B*). There are small low-density lesions in the right posterior frontal white matter and heavy calcification in the basal ganglia.

C and *D*, Axial T2 MR 18 months later, following progressive hemiparesis. There is extensive high signal in the posterior frontal white matter, extending through the gray matter adjacent to the convexity. There is also a small region of high signal in the occipital white matter.

associated with brain swelling, followed by atrophy (Fig. 27). Additional similar lesions occur with a generally progressive course.

Disorders of Amino Acid Metabolism, Maple Syrup Disease

This condition is due to deficiency of an enzyme necessary for the oxidative decarboxylation of keto acids, which are produced during the breakdown of the branch chain amino acids, leucine, isoleucine, and valine. The alpha-keto derivatives are partly transaminated and partly excreted in the urine, giving the characteristic maple syrup odor. The affected baby appears ill a few days after birth with vomiting and failure to thrive, followed by seizures and decreasing consciousness that may go on to coma. The head may be enlarged with widening of the sutures. Untreated survivors have severe brain damage with retardation, motor deficits, and blindness.

Evidence of onset in utero may be inferred from abnormalities of cerebral cortical cytoarchitecture implying defective neuronal migration, but the prominent features are generalized acute edema commencing a few days after birth and tending to subside after about 2 months, being replaced by atrophy. More characteristic, and

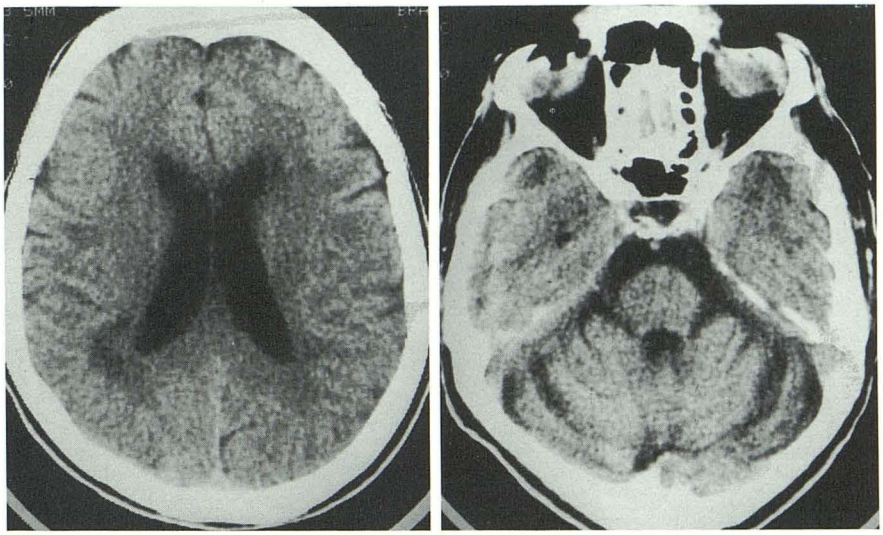

Fig. 25. MERRF; 50-year-old woman with progressive proximal weakness, myoclonus, and mild dementia. *A* and *B*, Axial CT; there is mild cerebral atrophy, marked cerebellar atrophy, and ill-defined low-density lesions in the cerebral white matter.

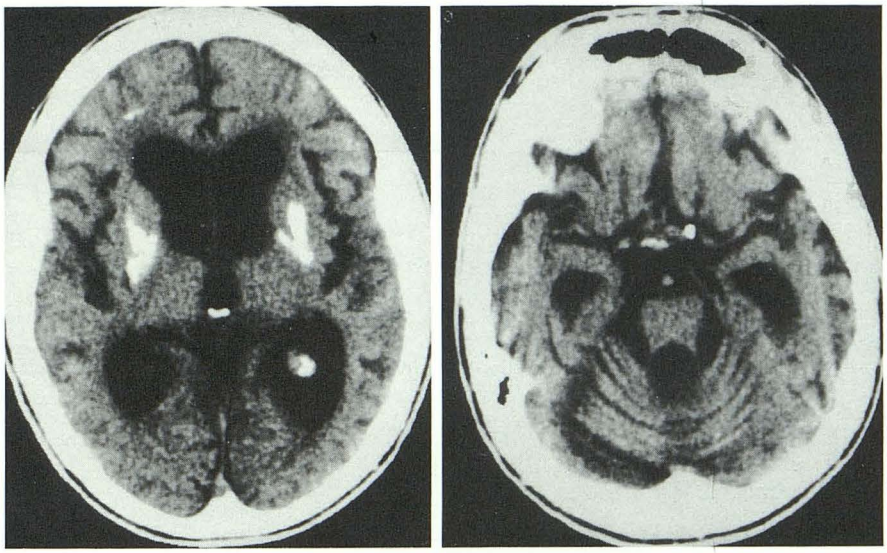

Fig. 26. Kearns-Sayre syndrome; 25-year-old man with long history of muscle weakness, cardiac conduction block, and external ophthalmoplegia. *A*, and *B*, Axial CT; there is marked cerebral, cerebellar, and brain stem atrophy with heavy calcification in the lentiform nuclei and faint calcification in the right frontal white matter.

perhaps pathognomonic, of the disease are spongiform changes, which are most prominent between about 3 and 8 weeks of age, involving the deep cerebellar white matter, dorsal brain stem, cerebral peduncles, and posterior limbs of the internal capsules. These changes may also decrease in severity, particularly with adequate therapy. Residual spongiform changes usually remain and tend to involve the medial longitudinal fasciculus and lateral lemniscus. Myelination is markedly delayed, particularly in the corticospinal tracts.

Imaging studies show no abnormality for the first few days of life (33). Then diffuse brain swelling is associated with white matter edema, which subsides before 2 months of age, leaving periventricular low density and signal change. The spongiform changes cause the characteristic more marked low density and altered signal in the deep cerebellar white matter, dorsal brain stem, cerebral peduncles, and dorsal parts of the internal capsule (Fig. 28), which subside after the second month, leaving symmetrical low density in the region of the lateral lemniscus.

Phenylketonuria

This autosomal recessive disorder occurs in up to about 1 in 10,000 of the population. It is usually due to deficiency of phenylalanine hydroxylase

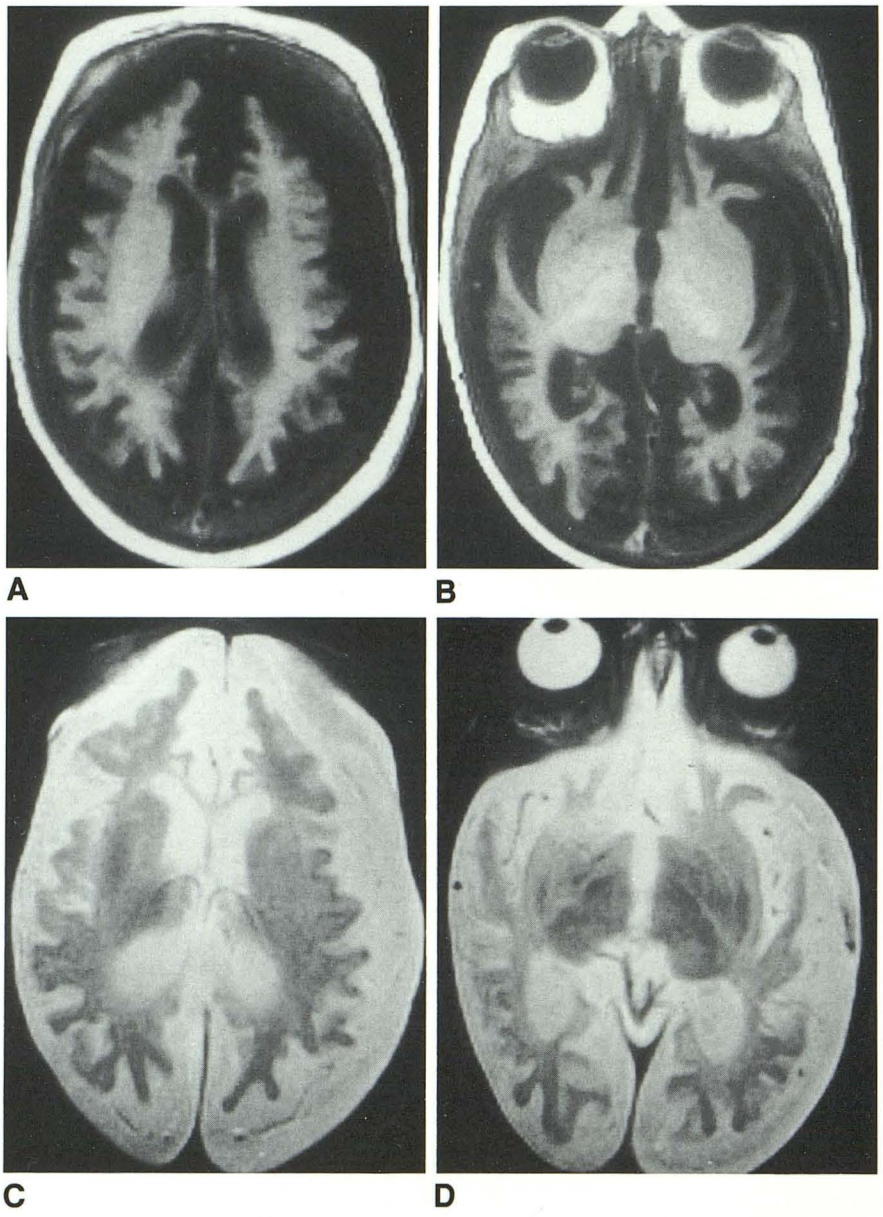

Fig. 27. Poliodystrophy; 1-year-old child with refractory convulsions and spasticity, gross mental retardation, and microcephaly. T1 MR (*A* and *B*) and T2 MR (*C* and *D*). There is marked cerebral atrophy, particularly affecting the cortex, with preservation of the basal ganglia. No abnormal signal changes are apparent.

that normally occurs in liver, kidney, and pancreas. Absence of phenylalanine hydroxylase inhibits conversion of the essential dietary amino acid phenylalanine to tyrosine. Tyrosine is essential for the manufacture of normal body protein. Phenylpyruvic and phenylacetic acids and phenylacetylglutamine are produced and excreted in the urine. These compounds are toxic to the brain particularly during development. They are associated with:

1. neuronal migration defects; and
2. delayed and defective myelination, particularly affecting the deep white matter of the cerebral hemispheres that may show spongiosis and gliosis. There is also diminished pigmentation, affecting hair coloring and the melanin contained in certain neurones, such as those of the substantia nigra.

Untreated children show mental and motor delay, with seizures, tremor, and microcephaly. Even with early treatment, there is evidence of mild intellectual deficit.

MR (34) shows signal changes that may be confined to and are most marked in the deep white matter adjacent to the trigones of the lateral ventricles. Signal abnormalities may also extend to involve all the deep periventricular white matter and be associated with cortical atrophy. The

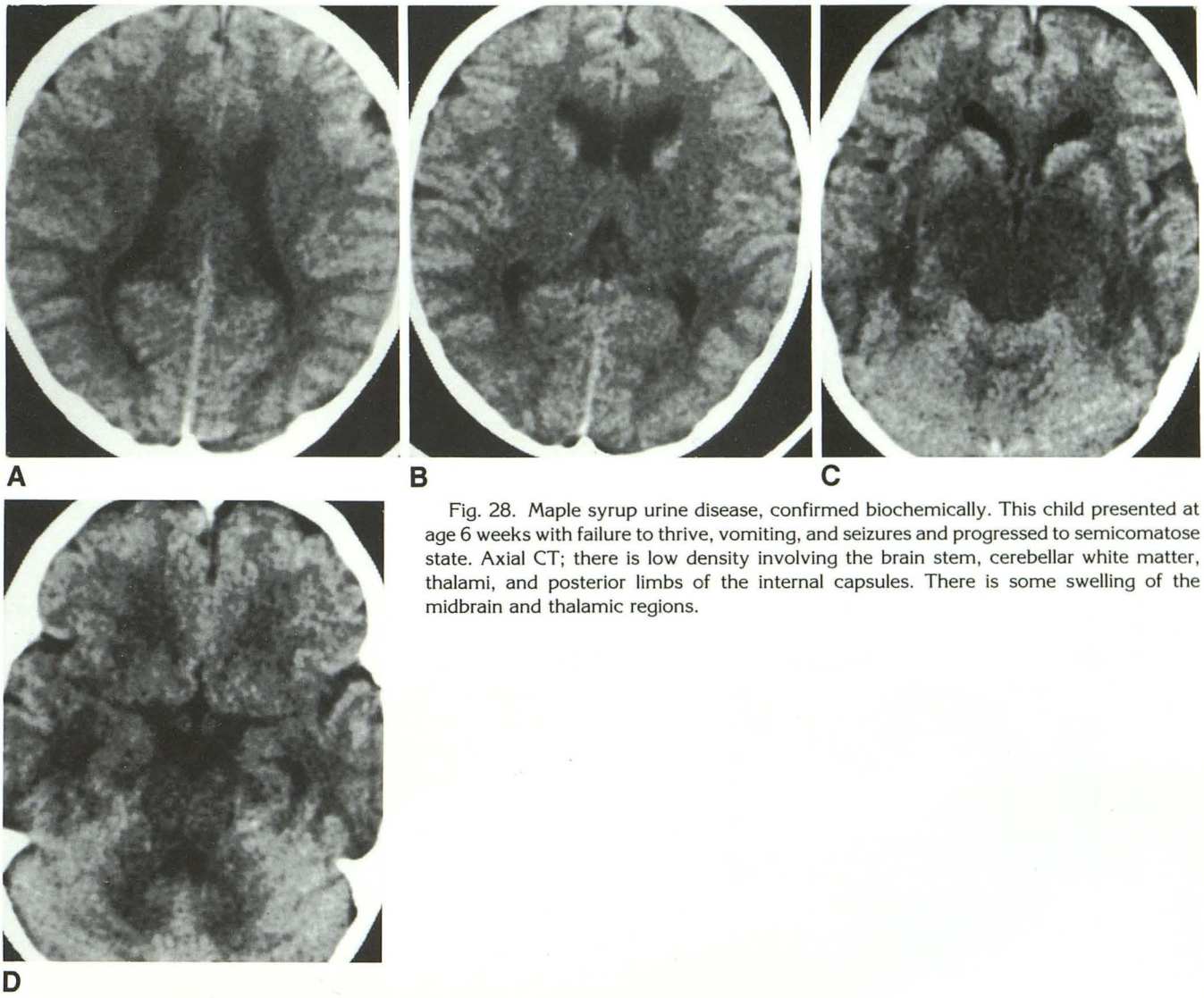

Fig. 28. Maple syrup urine disease, confirmed biochemically. This child presented at age 6 weeks with failure to thrive, vomiting, and seizures and progressed to semicomatose state. Axial CT; there is low density involving the brain stem, cerebellar white matter, thalami, and posterior limbs of the internal capsules. There is some swelling of the midbrain and thalamic regions.

radiologic changes do not correlate closely with the intelligence quotient nor with the efficacy of dietary regimes.

Neurologic deterioration has been observed in older children and young adults with phenylketonuria and has been associated with increasing abnormalities on MR (Fig. 29). These changes would correlate with foci of spongiosis, myelin breakdown, and gliosis, which have been noted on histopathology, but they have regressed on dietary therapy (35).

Hyperphenylalaninemia may also be associated with dihydropteridine reductase deficiency or with a defect in the biosynthesis of dihydrobiopterine due to tetramethyline hydrofolate reductase deficiency. This so-called malignant hyperphenylalaninemia manifests as mental retardation and convulsions from an early age. On computed imaging, the most characteristic appearance is calcification in the basal ganglia and cerebral subcortical white matter associated with atrophy (Fig. 30). Dysmyelination in the peritrigonal and parieto-occipital subcortical regions has caused signal changes on MR (36). These changes may be more widespread in the cerebral hemispheres and be associated with spongiform degeneration, which may also involve the brain stem and cerebellum.

Nonketotic Hyperglycinemia

This defect in the cleavage of glycine is associated with elevation of glycine level in the serum,

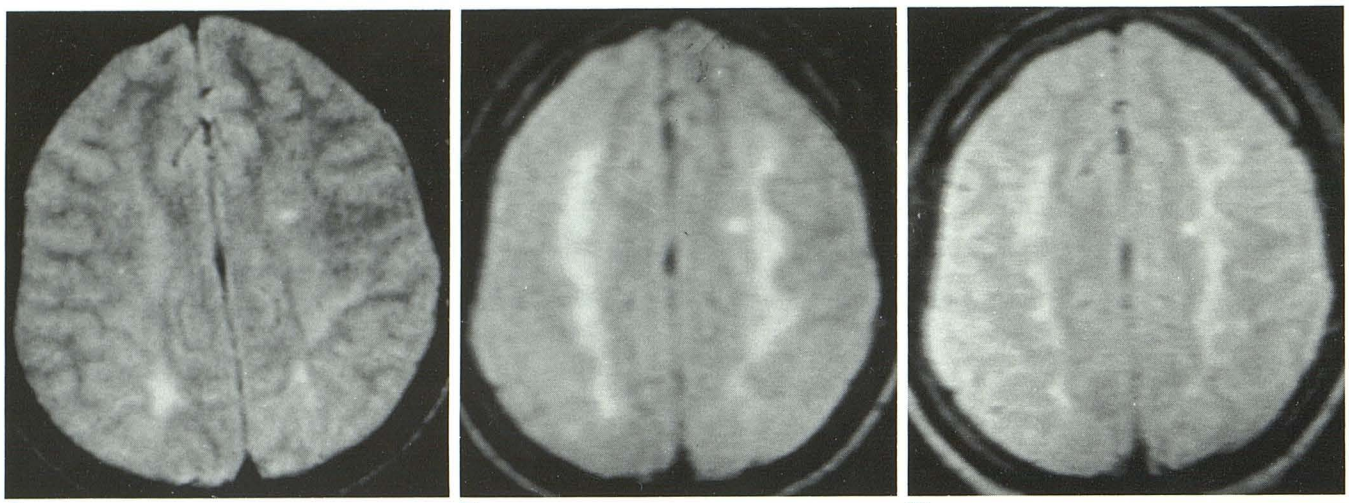

Fig. 29. Phenylketonuria.

Sequential axial T2 MR (Se 2060) at 23 years of age (*A*), when clinically stable, and at 25 years of age (*B*) following obvious clinical deterioration, show marked increase in the high signal in the frontal and parietal white matter.

C, After 2 months on a strict low phenylalanine diet, there is some regression of the high signal. (Reproduced with permission from *Lancet* (35).).

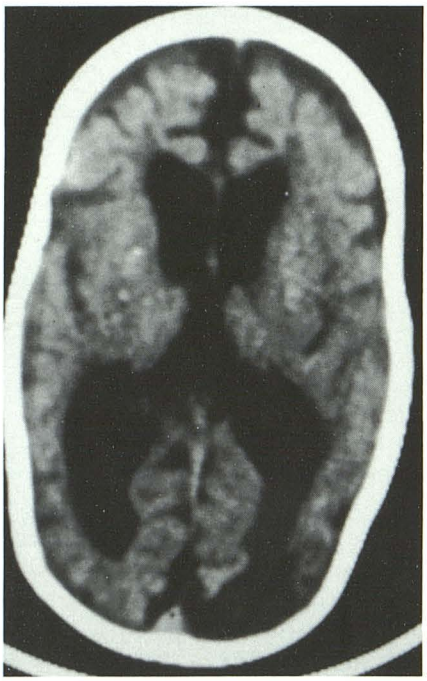

Fig. 30. Dihydropteridine reductase deficiency; 10-month-old boy retarded from birth. Axial CT; there is diffuse cerebral atrophy, calcification in the lentiform nuclei, and low density in the left occipital white matter.

CSF, and urine. It presents at, or soon after, birth with apneic episodes and hypotonia. There may be convulsions and myoclonus, and there is severe developmental delay with diminished head growth. Imaging studies (37) reflect the neuropathology. There is severe supra- and infratentorial atrophy, with thinning of the corpus callosum. Myelination is defective and delayed. Demyelination also occurs, accompanied by vacuolation, spongy degeneration, and gliosis of white matter, causing hypodensity with signal change on MR mainly in the periventricular regions. Partial and complete agenesis of the corpus callosum have been described.

Methylmalonic Acidemia (MMA) and Proprionic Acidemia (PA)

These conditions are associated with absence of the appropriate CoA carboxylases, which prevents conversion to succinate and results in ketoacidosis with excretion of the amino acids in the urine. Both diseases, but particularly proprionic acidemia, can present early with spastic quadriparesis and retardation. Imaging shows marked generalized atrophy. Patients with later onset of symptoms may make normal developmental progress but more commonly have a minor degree of retardation. Episodes of headache may be associated with metabolic acidosis and shock that result in neural damage, particularly involving the basal ganglia. CT may show low density in the cerebral white matter and/or the globi pallidi that may resolve or persist (Fig. 31). Signal change in the globi pallidi has been

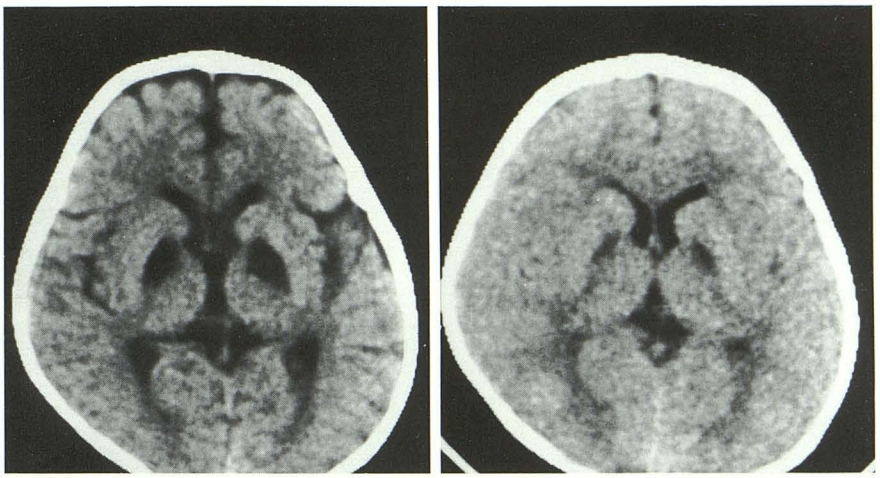

Fig. 31. Methylmalonic acidemia.
A, Axial CT at 1 year of age, following a bout of metabolic acidosis associated with profound shock. There is symmetrical low density in both globi pallidi and widening of cerebral sulci, suggesting brain shrinkage.
B, Cranial CT at age 3 years. The patient has very mild mental retardation, but is otherwise normal. The regions of low density in the basal ganglia are considerably smaller. The brain shrinkage has resolved.

noted on MR (Fig. 32) (38). In the early stages of methylmalonic acidemia, brain swelling may be present, but cerebral and cerebellar atrophy are usual.

Galactosaemia

This rare disorder is inherited as an autosomal recessive, most commonly due to galactose-1-phosphate uridyl transferase deficiency. It presents in the newborn or young infant with signs of raised intracranial pressure and vomiting, associated with cataracts, jaundice, and hepatosplenomegaly. Less commonly, galactosemia is caused by galactokinase deficiency, which tends to present later in infancy with similar symptoms. Both forms cause failure to thrive and mental retardation, and are associated with galactosuria. Neuroimaging may show extensive, but not specific, low density on CT (Fig. 33) and high signal throughout the hemispheric white matter on T2 MR. Diagnosis is by demonstrating the enzyme deficiencies in blood cells.

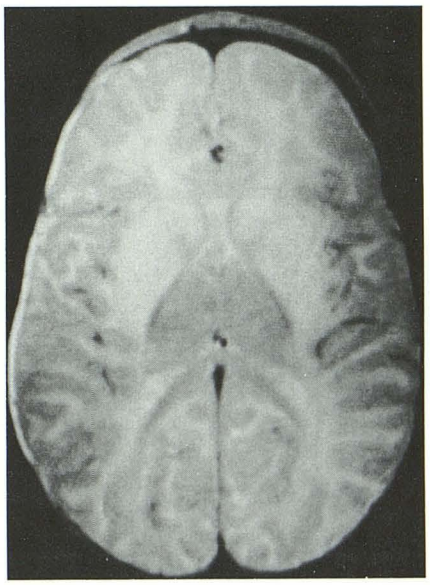

Fig. 32. Proprionic acidemia; 6-month-old boy with spastic quadriparesis and raised intracranial pressure. T2 MR; there is abnormally high signal in the caudate and lentiform nuclei. The ventricles appear small, consistent with brain swelling.

Methyl Group Transfer Abnormalities

Inborn errors of metabolism affecting cobalamin and folate through the methyl group transfer pathway include tetramethylene hydrofolate reductase and methionine adenosyl transferase deficiency. A common factor is a low CSF level of s-adenosyl methionine, which appears to be related to potentially reversible demyelination of central cerebral white matter shown on MR (Fig. 34).

Hyperammonemia

Urea Cycle Abnormalities. Several mitochondrial enzymes are involved in the urea cycle. Deficiency of any one of them may result in hyperammonemia that may be accentuated by high protein intake or intercurrent illness. The hyperammonemia results in intermittent cerebral dysfunction that may present as a movement disorder, seizures, confusion, or ataxia. The hyperammonemia is associated with spongiform

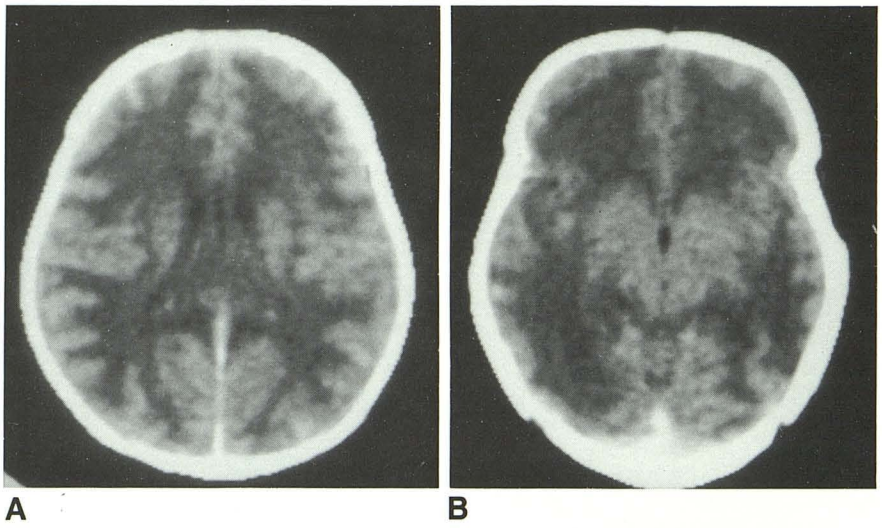

Fig. 33. Galactosaemia; 1-month-old girl with failure to thrive, vomiting, tense fontanelle, and cataracts. *A* and *B*, Axial CT; there is extensive, symmetrical, abnormally low density throughout the cerebral white matter. The ventricles are relatively small.

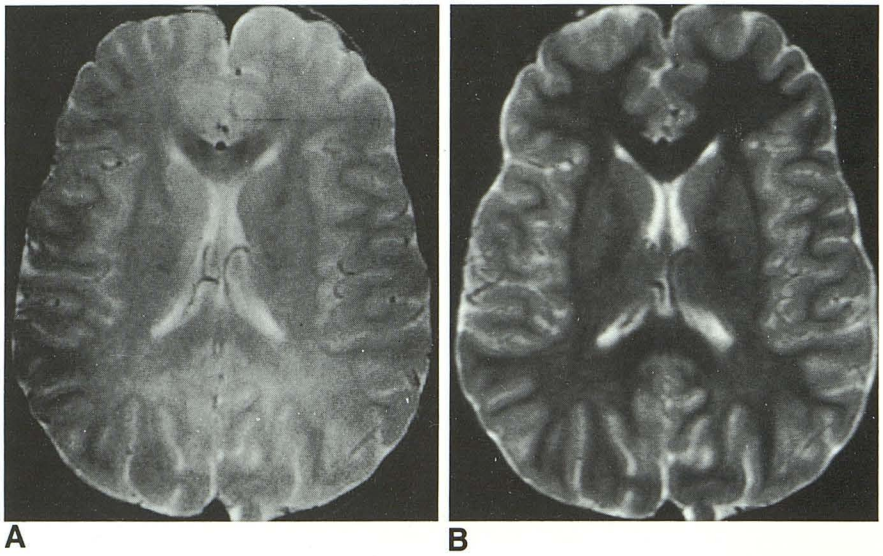

Fig. 34. Methionine adenosyl transferase deficiency; the patient first presented at age 1 year with failure to thrive and deafness.

A, At age 10 years the patient was mildly retarded and complained of headache but showed no neurologic signs. Axial T2 MR shows increased signal in the hemispheric white matter, including the internal capsules. The patient showed marked clinical improvement after treatment with oral s-adenosyl methionine.

B, Axial T2 MR at age 12 years. The white matter signal is now normal, suggesting that considerable myelination has taken place on treatment.

and cystic degeneration of the brain substance, accompanied by gliosis of the white matter and loss of neurones, which show as diffuse, at least partly reversible low density and high signal in the white matter on CT and T2W MR. These changes have been found in the recessively inherited conditions argininosuccinic aciduria and citrullinemia, as well as in the more common X-linked condition ornithine carbamyl transferase and carbamyl phosphate synthesase deficiencies. In these conditions, MR spectroscopy has shown high intracerebral levels of glutamine. Ornithine carbamyl transferase deficiency is peculiar in that it may present with severe stroke-like episodes that are associated with regions of diffuse involvement of gray and white matter resembling infarcts on CT and MR (Fig. 35). In advanced cases, atrophy is usual and often severe (Fig. 36).

Organic Acidurias. Glutamic aciduria type I results from deficiency of glutaryl-CoA-dehydrogenase, which is an essential enzyme in the catabolism of lysine, hydroxylysine, and tryptophan. It results in hyperammonemia and accumulation of glutaric acid, which causes metabolic acidosis and is excreted in increased amounts in the urine. Retarded and defective myelination is evident on MR. There is degeneration of the lentiform and caudate nuclei, which show low CT density and high T2 signal, plus evidence of atrophy (Fig. 37). Frontotemporal atrophy has been stressed as a feature of this

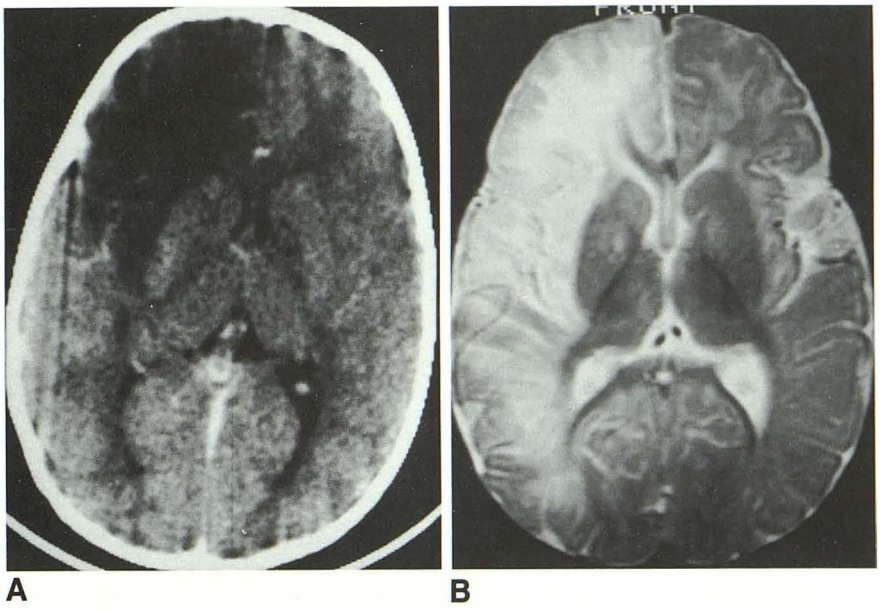

Fig. 35. Ornithine carbamyl transferase deficiency; 12-year-old girl with acute hemiplegia and convulsions.

A, Axial CT; there is extensive low density in the right frontal lobe, with moderate swelling.

B, T2 MR 4 days later shows extensive high signal in the right frontal and low right parietal white matter and increased signal in the left frontal white matter. The swelling is less marked.

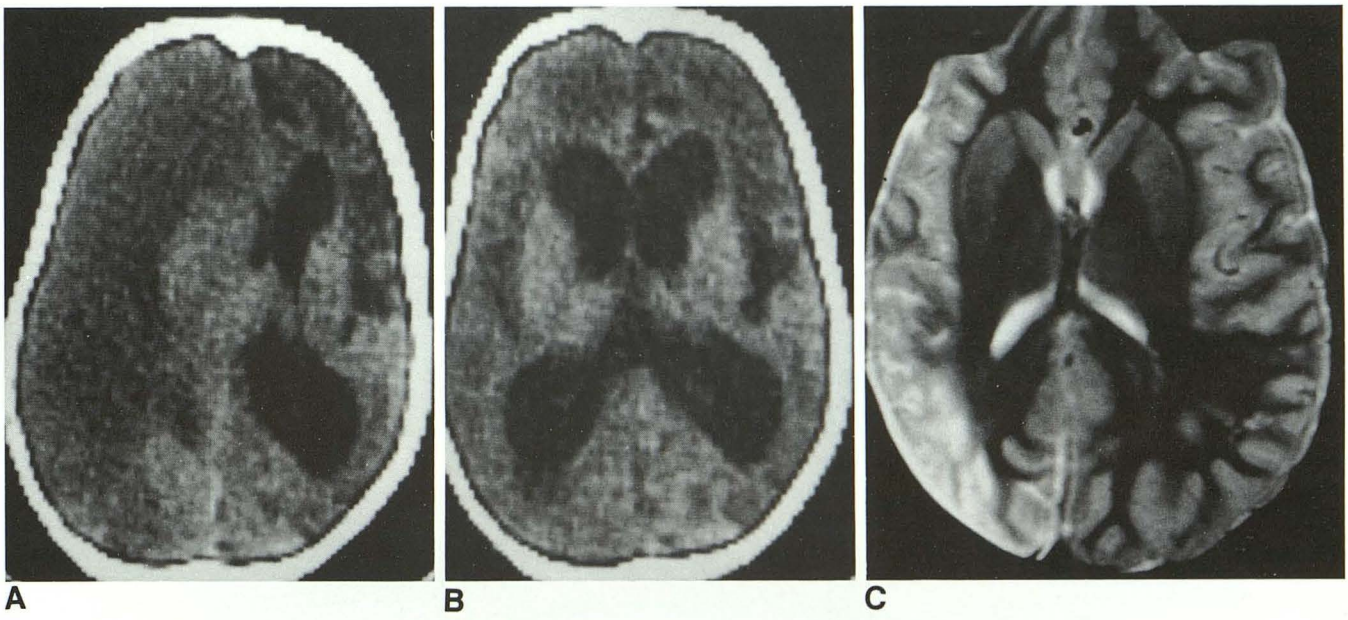

Fig. 36. Ornithine carbamyl transferase deficiency.

A, Axial CT at age 3 months, immediately following onset of hemiplegia. There is extensive low density and swelling in the white and gray matter of the right frontal and parietal lobes, with compression of the right lateral ventricle. There is low density in the left frontal lobe, left sided atrophy, and dilatation of the left lateral ventricle.

B, Axial CT 6 weeks later, shows progression of atrophy, especially on the right. There is interval resolution of much of the low density, but some low density persists in both frontal lobes.

C, Axial T2 MR of the same patient at age 11 years shows marked right hemiatrophy, high signal in the cortex and most of the white matter of the right hemisphere, and small foci of high signal in the left parietal white matter.

condition, which is manifest particularly in widening of the Sylvian fissures. External hydrocephalus has also been described with extracerebral fluid and enlargement of the cranial vault (Fig. 38) (39).

Cystinuria usually presents with life-threatening renal failure. In survivors, crystals may be precipitated in the choroid plexuses, and necrosis has been described affecting the internal capsules. Homocystinuria, usually due to cystathio-

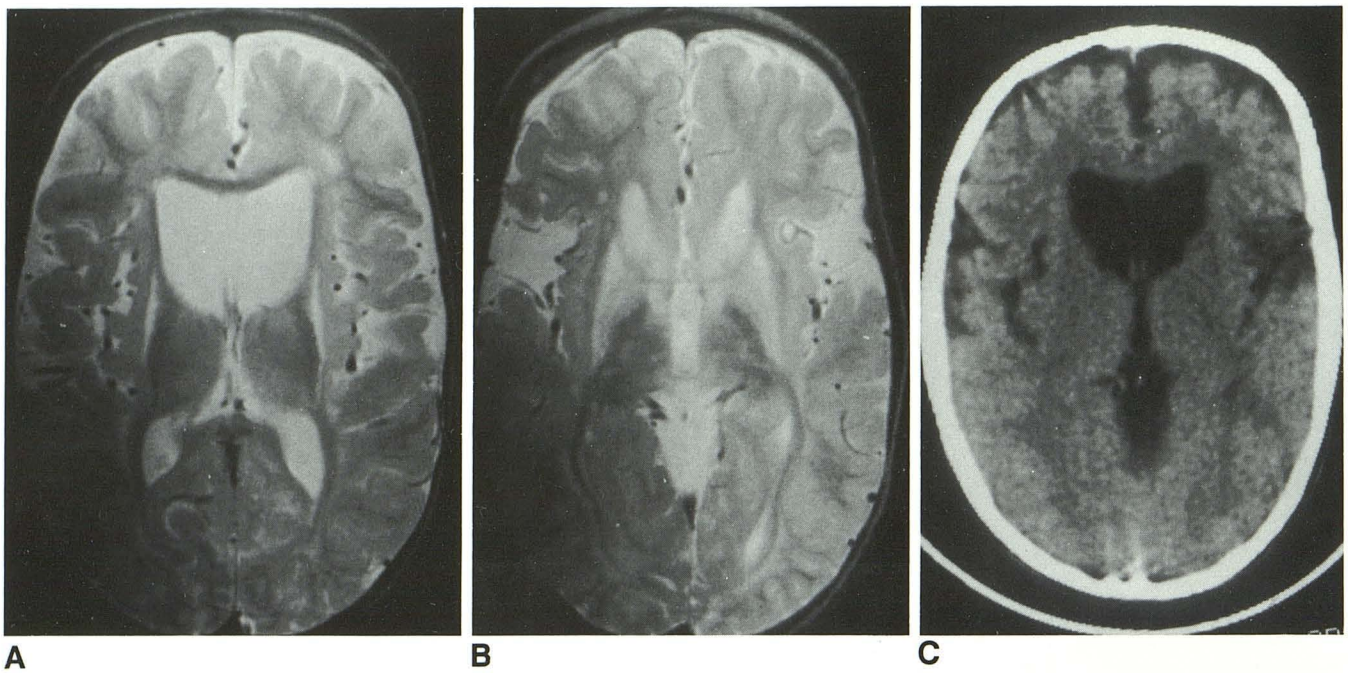

Fig. 37. Glutaric aciduria, type 1; 5-year-old boy with retarded development.

A and *B*, Axial T2 MR; there is abnormally high signal in the caudate and lentiform nuclei, and in the deep cerebral white matter. There is enlargement of the frontal horns and of the subarachnoid spaces over the frontal lobes, and considerable dilatation of the Sylvian fissures.

C, Axial CT, the atrophy is evident, particularly in the caudate nuclei. There are small low-density lesions in the lentiform nuclei, but these abnormalities are much less evident than on MR.

Fig. 38. Glutaric aciduria, type 1; 7-year-old boy with mental retardation and enlargement of the cranial vault. *A* and *B*, Cranial CT; there is a small region of low density in the left lentiform nucleus and mild enlargement of the lateral ventricles. The Sylvian fissures are widened and there are accumulations of extracerebral fluid over the convexities of both hemispheres, expanding the adjacent vault.

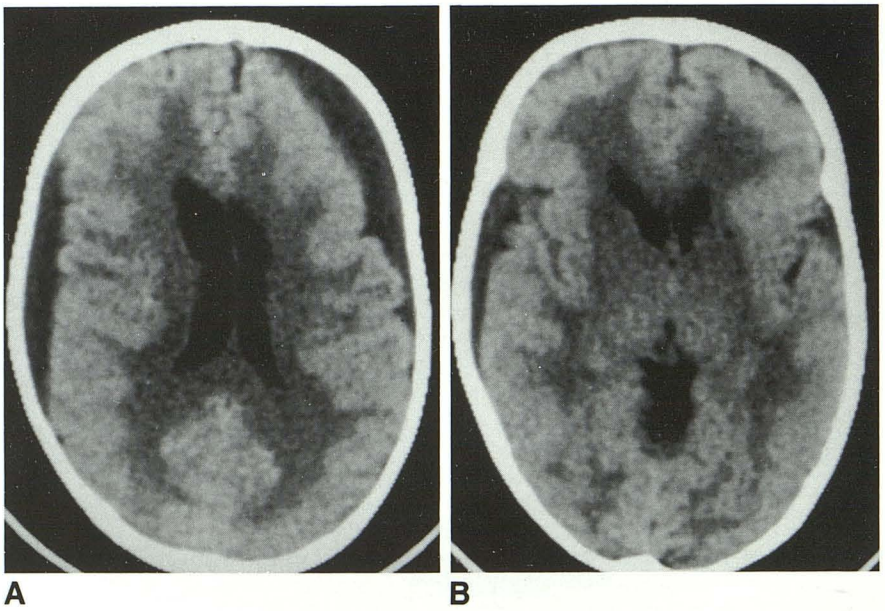

nine beta-synthase deficiency, commonly presents at 6–9 months of age with focal ischaemia due to cerebrovascular occlusion, or with seizures and retardation. Computed imaging may reveal infarction and/or atrophy.

Deficiency of 3-hydroxy-3-methylglutaryl-CoA-lyase is an extremely rare disorder, presenting in the first few months of life with evidence of acidosis and hyperammonemia. There is intellectual and motor delay, with clumsiness and

ataxia, intention tremor, and macrocephaly. The diagnosis is made by showing deficiency in leukocytes of the enzyme that is necessary for the metabolism of leukine. There is spongiform degeneration of the white matter, sometimes associated with large cystic spaces. The changes on CT and MR simulate Canavan disease (40).

Many less common disorders of catabolism of branched amino acids and organic acids are recognized, and may be found during screening of the mentally retarded and of infants who fail to thrive. In some of these disorders, computed imaging is unnecessary or unremarkable, but in others, striking, usually symmetrical, abnormalities are evident (Fig. 39).

Trichopoliodystrophy (Menkes Disease)

This is an X-linked condition related to a diminished absorption of copper from the alimentary tract and a diminished level of serum ceruloplasmin. It decreases the function of copper-dependent enzymes, including cytochrome oxidase, but the primary disease process is almost certainly a mitochondrial enzyme defect. The disease presents in the neonatal period with failure to thrive, fits, and developmental delay, and death occurs in 4–6 months. The hair, originally normal, becomes colorless, friable, and kinky. The arteries are tortuous and elongated with splits in the intima, resulting in irregularity of the lumina. The long bones show metaphyseal spurring and diaphyseal periosteal reaction that has been mistaken for the results of injury. The skull shows an increased number of wormian bones.

There is degeneration of cerebral and cerebellar gray matter, with neuronal loss, fibrillary gliosis, patchy necrosis, and cystic change leading to rapid atrophy (Fig. 40). Focal regions of low density may be present on CT, suggesting infarcts (Fig. 41). Subdural bleeding from dilated meningeal vessels may cause subdural effusions of low or high density.

Conclusion

There can be little doubt that many other metabolic disorders will eventually be shown to fall within this classification. They have been omitted, however, because the precise nature of their underlying inherited metabolic defects has not yet been elucidated. Some of these conditions, including Alexander disease (41), Pelizaeus-Merzbacher disease (42), and Cockayne syndrome (43, 44) cause characteristic changes on computed imaging. Others, such as familial pro-

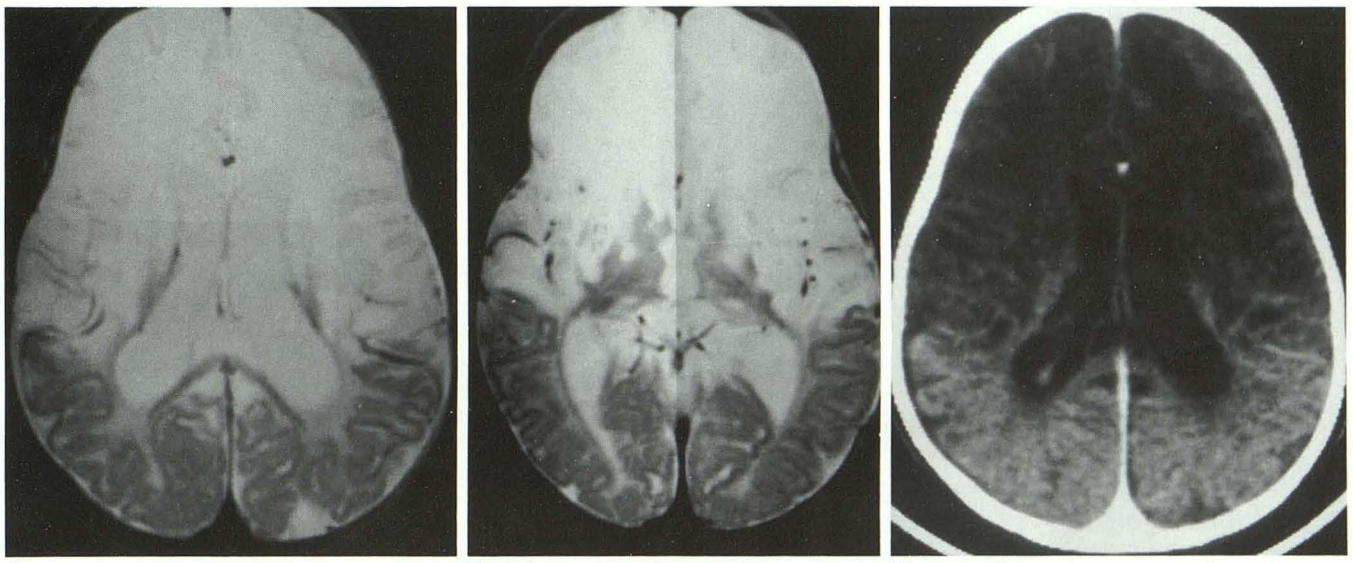

Fig. 39. Deficiency of branch chain ketoacid dehydrogenase complex; infant with severe ketoacidosis and seizures, progressing to respiratory irregularity and failure leading to coma and death.

A and *B*, Axial T2 MR; there is marked increase in signal throughout the frontal and the anterior halves of the temporal lobes, also involving the caudate and lentiform nuclei.

C, Axial CT shows low density in the same regions, and mild ventricular dilatation.

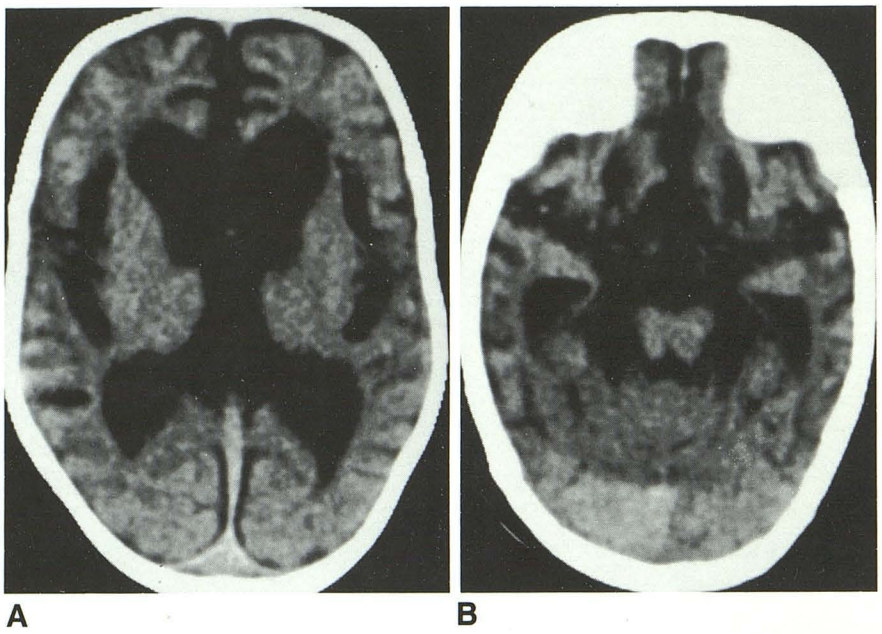

Fig. 40. Menkes disease; 6-month-old boy with mental retardation and spasticity. *A* and *B*, Cranial CT; there is severe diffuse atrophy of the cerebral hemispheres, deep gray nuclei, and brain stem.

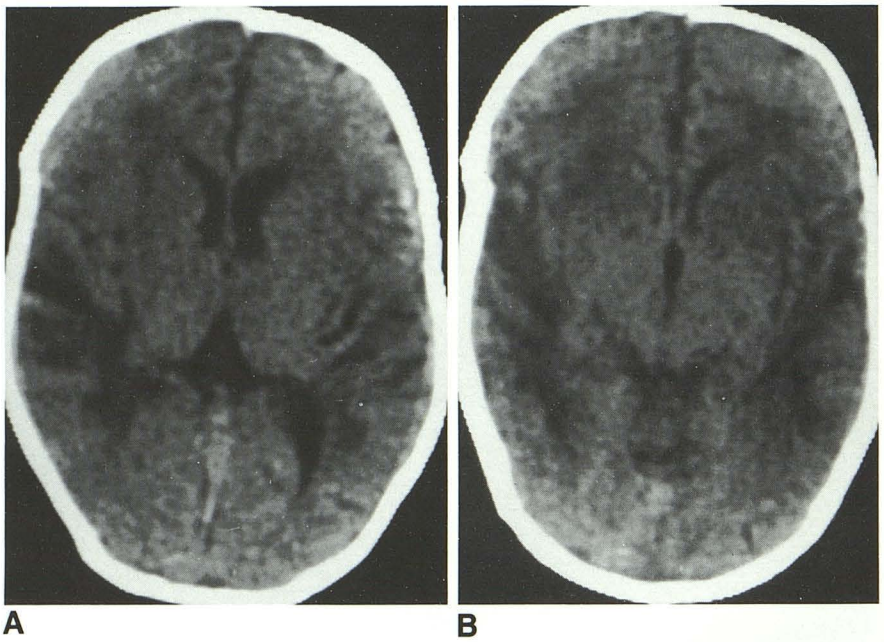

Fig. 41. Menkes disease; 2-month-old boy. *A* and *B*, Cranial CT; there are low-density lesions in the white matter and cortex of both temporal lobes, and ill-defined regions of low density in the frontal white matter and basal ganglia bilaterally. Such lesions are associated with ischemic events secondary to the arterial abnormalities.

gressive myoclonic epilepsy, with or without Lafora bodies, exhibit only nonspecific changes, predominantly atrophy.

Diagnosis will remain in the realm of biochemistry, but imaging has a significant role in management and in suggesting the diagnosis in cases presenting with atypical clinical features.

References

1. Valk J, van der Knaap MS. *Magnetic resonance of myelin, myelination, and myelin disorders.* New York: Springer-Verlag, 1989:82
2. Demaerel P, Wilms G, Verdru P, Carton H, Baert AL. MR findings in globoid leukodystrophy. *Neuroradiology* 1990;32:520–522
3. Morgan SH, Rudge P, Smith SJM, et al. The neurological complications of Anderson-Fabry disease (alpha-galactosidase A deficiency): investigation of symptomatic and presymptomatic patients. *Q J Med* 1990;75:491–504
4. Brismar J, Brismar G, Coates R, Gascon G, Ozand P. Increased density of the thalamus on CT scans in patients with GM2 gangliosidoses. *AJNR* 1990;11:125–130
5. Dietemann JL, Filippide la Palavesa MM, Tranchant C, Kastler B. MR findings in mannosidosis. *Neuroradiology* 1990;32:485–487
6. Echenne B, Divry P, Vianey-Liaud C. Spongy degeneration of the neuraxis (Canavan-Van Bogaert disease) and N-acetylaspartic aciduria. *Neuropediatrics* 1989;20:79–81

7. Harbord MG, Harden A, Harding B, Brett EM, Baraitser M. Megalencephaly with dysmyelination, spasticity, ataxia, seizures and distinctive neurophysiological findings in two siblings. *Neuropediatrics* 1990;21:164–168
8. Brismar J, Brismar G, Gascon G, Ozand P. Canavan's disease: CT and MR imaging of the brain. *AJNR* 1990;11:805–810
9. Savolaine ER, Voeller K, Gunning W, Smith RR. Computed tomography in neuronal ceroid lipofuscinosis: four case reports. *CT J Comput Tomogr* 1987;11:73–78
10. Raininko R, Santavouri P, Heiskala H, Sainio K, Palo J. CT findings in neuronal ceroid lipofuscinoses (NCL). *Neuropediatrics* 1990;21:95–101
11. Machen BC, Williams JP, Lum GB, et al. Magnetic resonance imaging in neuronal ceroid lipofuscinosis. *CT J Comput Tomogr* 1987;11:160–166
12. Wanders RJA, Van Roermund CWT, Schutgens RBH. The inborn errors of peroxisomal beta-oxidation: a review. *J Inherited Metab Dis* 1990;13:4–36
13. Baker RH, Trautmann JC, Younge BR, Nelson Kent D, Zimmerman D. Late juvenile-onset Krabbe's disease. *Ophthalmology* 1990;97:1176–1180
14. Uchiyama M, Hata Y, Tada S. MR imaging in adrenoleukodystrophy. *Neuroradiology* 1991;33:25–29
15. van der Knaap MS, Valk J. The MR spectrum of peroxisomal disorders. *Neuroradiology* 1991;33:30–37
16. Poll-The BT, Roels F, Ogier M, Scotto J. A new peroxisomal disorder with enlarged peroxisomes and a specific deficiency of acyl-CoA oxidase pseudoneonataladrenoleukodystrophy. *Am J Hum Genet* 1988;42:422–434
17. Berginer VM, Berginer J, Salen G, Shefer S, Zimmerman RD. Computed tomography in cerebrotendinous xanthomatosis. *Neurology* 1981;31:1463–1465
18. Williams DW, Elster AD, Cox TD. Cranial MR imaging in rhizomelic chondrodysplasia punctata. *AJNR* 1991;12:363–365
19. Lee BCP, Martens M. Mitochondrial respiration and energy metabolism in muscle. In: Engel A, Benker B, eds. *Myology.* New York: McGraw-Hill, 1986:643–671
20. Morgan-Hughes JA. Mitochondrial myopathies. In: Mastalgia FL, Walton J, eds. *Skeletal muscle pathology.* Edinburgh: Churchill Livingstone, 1982:309–339
21. Ishitsu T, Miike T, Kitano A, et al. Heterogeneous stereotypes of mitochondrial encephalopathy in a single kindred. *Neurology* 1987;37:1867–1869
22. Yamagata T, Sadayuki Y, Okabe I, et al. Ultrasonography and magnetic resonance imaging in Leigh disease. *Paediatr Neurol* 1990;6:326–329
23. Suzuki T, Koizumi J, Shiraishi H, et al. Mitochondrial encephalomyopathy (MELAS) with mental disorder: CT, MRI and SPECT findings. *Neuroradiology* 1990;32:74–76
24. Rosen L, Phillips S, Enzmann D. Magnetic resonance imaging in MELAS syndrome. *Neuroradiology* 1990;32:168–171
25. Hasuo K, Tamura S, Yasumori K, et al. Computed tomography and angiography in MELAS (mitochondrial myopathy, encephalopathy, lactic acidosis, and stroke-like episodes): report of 3 cases. *Neuroradiology* 1987;29:393–397
26. Taverni N, Dal Pozzo G, Arnetoli G, Zappoli R. Diagnosis and follow up of mitochondrial encephalomyopathy: CT and MR studies. *J Comput Assist Tomogr* 1988;12:696–697
27. Abe K, Inui T, Hirono N, Mezaki T, Kobayashi Y, Kameyama M. Fluctuating MR images with mitochondrial encephalopathy, lactic acidosis, stroke-like syndrome (MELAS). *Neuroradiology* 1990;32:77
28. Allard JC, Tilak S, Carter AP. CT and MR of MELAS syndrome. *AJNR* 1988;9:1234–1238
29. Oldfors A, Fyhr IM, Holme E, Larsson NG, Telinius M. Neuropathology of Kearns-Sayre syndrome. *Acta Neuropathol* 1990;80:541–546
30. Demange P, Gia HP, Kalifa G, Sellier N. MR of Kearns-Sayre syndrome. *AJNR* 1989;10:S91
31. Heimann-Patterson TD, Bonilla E, DiMauro S, Foreman J, Schotland DL. Cytochrome-c-oxidase in a floppy infant. *Neurology* 1982;32:898–900
32. Prick MJJ, Gabreels FIM, Renier WO, Trijbels JMF, Sengers RCA, Slooff JL. Progressive infantile poliodystrophy: association with disturbed pyruvate oxidation in muscle and liver. *Arch Neurol* 1981;38:767–772
33. Brismar J, Aqeel A, Brismar G, Coates R, Gascon G, Ozand P. Maple syrup urine disease. *AJNR* 1990;11:1219–1228
34. Pearson KD, Gean-Marton AD, Levy HL, Davis KR. Phenylketonuria: MR imaging of the brain with clinical correlation. *Radiology* 1990;177:437–440
35. Thompson AJ, Smith I, Brenton D, et al. Neurological deterioration in young adults with phenylketonuria. *Lancet* 1990;336:602–605
36. Sugita R, Takahashi S, Ishii K, et al. Brain CT and MR findings in hyperphenylalaninaemia due to dihydropteridine reductase deficiency (variant of phenylketonuria). *J Comput Assist Tomogr* 1990;14:699–703
37. Press GA, Barshop BA, Haas RH, Nyhan WL, Glas RF, Hesselink JR. Abnormalities of the brain in non-ketotic hyperglycinaemia. *AJNR* 1989;10:315–321
38. Korf B, Wallman JK, Levy HL. Bilateral lucency of the globus pallidus complicating methylmalonic acidaemia. *Ann Neurol* 1986;20:364–366
39. Mandel H, Braun J, El-Peleg O, Christiansen B, Berant M. Glutaric aciduria type I. *Neuroradiology* 1991;33:75–78
40. Lisson G, Leupold D, Bechinger D, Wallesch C. CT findings in a case of deficiency of 3-hydroxy-3-methylglutaryl-CoA-lyase. *Neuroradiology* 1981;22:99–101
41. Holland IM, Kendall BE. Computed tomography in Alexander's disease. *Neuroradiology* 1980;20:103–106
42. Scheffer IE, Baraitser M, Wilson J, Harding B, Kendall B, Brett EM. Pelizaeus-Merzbacher disease: classical or connatal? *Neuropediatrics* 1991;22:71–78
43. Boltshauser E, Yalcinkaya C, Wichmann W, Reuter F, Prader A, Valavanis A. MRI in Cockayne syndrome type I. *Neuroradiology* 1989;31:276–277
44. Demaerel Ph, Wilms G, Verdru P, Carton H, Baert AL. MRI in the diagnosis of Cockayne syndrome. *J Neuroradiol* 1990;17:157–160